Electronic Supplementary Material (ESI) for Dalton Transactions.

SUPPORTING INFORMATION

The synthesis, characterisation and application of iron(III)-acetate complexes for cyclic carbonate formation and the polymerisation of lactide

Oliver J. Driscoll,Claudia H. Hafford-Tear, Paul McKeown, Jack A. Stewart, Gabriele Kociok-Köhn, Mary F. Mahon and Matthew D. Jones[]*

[a] *Department of Chemistry, University of Bath, Claverton Down, Bath, BA2 7AY, UK*

General considerations

All chemicals were commercially obtained from Sigma-Aldrich and used as received. This is with the exception of the *rac*-lactide, which was singly recrystallised from dry toluene. Cyclohexene oxide (CHO), propylene oxide (PO), styrene oxide (SO), epichlorohydrin (ECH), phenyl glycidyl ether (PGE) and allyl glycidyl ether (AGE) were stirred with CaH_2, cannula filtered and distilled before use. Benzyl alcohol and trimethylamine were distilled before use. For anhydrous conditions and CO_2 / epoxide coupling reaction preparation, an MBraun LABmaster dp glovebox, standard Schlenk line techniques and oven-dried glassware were used. The Fe(III) complexes were synthesised in air and, together with all reagents used for polymerisations and CO_2 / epoxide coupling reactions, stored in the MBraun LABmaster dp glovebox.

NMR spectroscopy of the polymerisations, crude cyclic carbonate reaction mixtures and Evans method were recorded on Bruker 400 II MHz or 500 MHz Spectrometer instruments and referenced to residual solvent signals. Polymerisation conversion was recorded from the integration of the methine region of the polymer (δ 5.12 - 5.20 ppm) against that of the monomer (δ 4.94 – 5.01). The tacticity of polymers was determined from its ^1H {^1H} NMR spectrum, decoupling from the polymer doublet at δ 1.62 ppm. ^1H {^1H} NMR was recorded on a Bruker AV 400 MHz spectrometer. Ligands were prepared and characterised following previously reported literature.[1–3] All Fe(III) complexes were characterised by electrospray ionisation-mass spectrometry (ESI-MS) using a MicroToF electrospray quadrupole time-of-flight mass spectrometer, with the sample dissolved in acetonitrile at approximately 1 μgmL^{-1} concentration. Mass spectra were recorded in positive loop injection mode set for a range of 50 - 1500 m/z. Elemental analysis was performed by Elemental Microanalysis Ltd.

Ultraviolet-visible spectroscopy (UV-Vis) was performed using an Agilent Technologies Cary60 Spectrophotometer and Cary WinUV software. The samples were analysed in acetonitrile solvent and absorbance recorded between 300 – 800 nm. Fourier-transform infrared spectroscopy (FT-IR) was performed using a PerkinElmer Spectrum 100 FT-IR Spectrometer. The pressurised CO_2 / epoxide coupling reactions were performed using a Parr 5500 Series Compact Reactor with mechanical stirring and a Parr 4848 Reactor Controller for temperature control. Evans' NMR spectroscopic method was conducted in $CDCl_3$ solvent using a capillary of pure $CDCl_3$, Bruker 400 II MHz or 500 MHz Spectrometers generally at 298 K and taking into account the mass susceptibility of $CDCl_3$ and diamagnetic contribution of all atoms.

MALDI-ToF analysis was carried out on a Bruker Autoflex speed instrument in reflector positive mode, using DCTB as the matrix at a concentration of 10 mg mL^{-1}. 50 µL of this solution was co-applied with 2 µL of 0.1 M NaTFA solution and 10 µL of the analyte at a concentration of 10 mg mL^{-1}. 1 µL of this homogenised solution was applied to a steel target plate for analysis. Materials characterization (GPC, MALDI-ToF) facilities were provided through MC^2 at the University of Bath.

Powder X-ray diffraction data was collected on a STOE Stadi P, using Cu radiation (1.540598 Å) and a Multi-MYTHEN detector, in transmission mode. All single crystallographic data was collected on either a SuperNova or Excalibur, EOS detector diffractometer using CuKα (λ = 1.54184 Å) or Mo-Kα (λ = 0.71073 Å) radiation. All data was recorded at 150(2) K. All structures were solved by direct methods and refined on all F^2 data using the SHELXL-2014 suite of programs. All hydrogen atoms were included in idealised positions and refined using the riding model, all refinement details are given in the .cif file. CCDC numbers 1940647-1940654 contains the necessary crystallographic data. Refinement was generally straightforward with the following exceptions:

Fe(**2**)OAc: Two molecules of disordered ethanol in unit cell with occupancies of 50% each.

Fe(**3**)OAc: Two molecules of ethanol in unit cell with partial occupancy (50%).

Fe(**6**$_{\boldsymbol{RR}}$)Y_2: The asymmetric unit comprises half of one molecule. The remainder can be generated *via* the 2-fold rotation axis on which the iron centre is located. (This axis also travels through the midpoint between C_3 and its symmetry equivalent). It became obvious quite early in the refinement process that the ligand based on O2 is disordered, and this has been modelled as 2 acetate components (with fractional occupancies of 30% and 35%) and one one ethoxy substituent (with an occupancy of 35%). Chemically, one of these disordered entities in the asymmetric unit must be protonated 50% of the time. However, the disorder level precluded inclusion of any such credibly located fractional hydrogen - and it was therefore omitted from the refinement. Some distance and ADP restraints were employed in the disordered region, to assist convergence.

Fe(**8**)OAc: The void contains a string of 4 heavily disordered partially occupied EtOH molecules. Another disordered EtOH molecule could be found in the proximity of N3 summing it up to 3 EtOH.

General complexation procedure for Fe(X)OAc under air

$Fe(OAc)_2$ (0.174 g, 1.0 mmol) was placed in a round bottom flask in the glovebox. In air, ethanol (10 mL) was added to the $Fe(OAc)_2$ to form a brown suspension. The ligand (1.0 mmol) was added as a solid to this mixture and refluxed for 2.5 hours and left to cool to room temperature. After Büchner filtration and rinsing with cold ethanol, the final product was isolated and dried.

Complex Characterisation

Fe(2)Cl: Reported and used in previous literature.[4]

Fe(1)OAc: Yield = 0.292 g, 57%. ESI-MS (MeCN): Calcd *m/z* $[C_{25}H_{34}FeN_2O_2]^+$ = 450.1970, found *m/z* = 450.2099. Elemental analysis: Calcd for $C_{27}H_{37}FeN_2O_4$ + EtOH (found): C, 62.70 (60.96), H, 7.80 (7.99), N, 5.04 (5.02). FT-IR: 3673 cm^{-1} (O-H (alcohol), solvent), 2988 cm^{-1}, 2962 cm^{-1}, 2905 cm^{-1} (C-H (alkyl)), 1630 cm^{-1} (C=N), 1598 cm^{-1}, 1551 cm^{-1}, 1472 cm^{-1}, 1447 cm^{-1}, 1408 cm^{-1}, 1394 cm^{-1} (C=C (Ar), C=O (acetate)). Effective magnetic moment = 5.21 μ_B at 297 K in $CDCl_3$.

Fe(2)OAc: Yield = 0.238 g, 38%. ESI-MS (MeCN): Calcd *m/z* $[C_{33}H_{50}FeN_2O_2]^+$ = 562.3222, found *m/z* = 562.3252. Elemental analysis: Calcd for $C_{35}H_{53}FeN_2O_4$ + EtOH (found): C, 66.56 (65.85), H, 8.91 (8.89), N, 4.20 (4.36). FT-IR: 2954 cm^{-1}, 2901 cm^{-1}, 2866 cm^{-1} (C-H (alkyl), 1619 cm^{-1} (C=N), 1536 cm^{-1}, 1459 cm^{-1}, 1441 cm^{-1}, 1412 cm^{-1} (C=C (Ar), C=O (acetate)). Effective magnetic moment = 5.74 μ_B at 298 K in $CDCl_3$.

Fe(3)OAc: Yield = 0.419 g, 61%. ESI-MS (MeCN): Calcd *m/z* $[C_{38}H_{52}FeN_2O_2]^+$ = 624.3378, found *m/z* = 624.3488. Elemental analysis: Calcd for $C_{40}H_{55}FeN_2O_4$ + EtOH (found): C, 69.12 (67.56), H, 8.43 (8.20), N, 3.84 (3.90). FT-IR: 3415 cm^{-1} (O-H (alcohol), solvent), 2961 cm^{-1}, 2949 cm^{-1}, 2901 cm^{-1}, 2865 cm^{-1} (C-H (alkyl)), 1620 cm^{-1} (C=N), 1537 cm^{-1} (C=C (Ar), C=O (acetate)). Effective magnetic moment = 5.25 μ_B at 298 K in $CDCl_3$.

Fe(4)OAc: Yield = 0.359 g, 54%. ESI-MS (MeCN): Calcd *m/z* $[C_{36}H_{54}FeN_2O_2]^+$ = 602.3535, found *m/z* = 602.3549. Elemental analysis: Calcd for $C_{38}H_{57}FeN_2O_4$ (found): C, 68.97 (69.21), H, 8.68 (8.86) N, 4.23 (4.36). FT-IR: 2951 cm^{-1}, 2940 cm^{-1}, 2905 cm^{-1}, 2868 cm^{-1} (C-H (alkyl)), 1621 cm^{-1} (C=N), 1618 cm^{-1}, 1538 cm^{-1}, 1457 cm^{-1}, 1437 cm^{-1}, 1411 cm^{1} (C=C (Ar), C=O (acetate)). Effective magnetic moment = 5.46 μ_B at 297 K in $CDCl_3$.

Fe(5)OAc: Yield = 0.319 g, 50%. ESI-MS (MeCN): Calcd *m/z* $[C_{34}H_{52}FeN_2O_2]^+$ = 576.3378, found *m/z* = 576.3464. Elemental analysis: Calcd for $C_{36}H_{55}FeN_2O_4$ (found): C, 68.02 (64.75), H, 8.72 (8.45), N, 4.41 (4.31). FT-IR: 3581 cm^{-1} (O-H (alcohol), solvent), 2950 cm^{-1}, 2905 cm^{-1}, 2871 cm^{-1} (C-H (alkyl)), 1611 cm^{-1}(C=N), 1541 cm^{-1}, 1467 cm^{-1}, 1438 cm^{1}, 1415 cm^{-1} (C=C (Ar), C=O (acetate)). Effective magnetic moment = 4.57 μ_B at 298 K in $CDCl_3$.

Fe(6*meso*)OAc: Yield = 0.278 g, 53%. ESI-MS (MeCN): Calcd *m/z* $[C_{26}H_{34}FeN_2O_2]^+$ = 462.1970, found *m/z* = 462.2006. Elemental analysis: Calcd for $C_{28}H_{37}FeN_2O_4$ + EtOH (found): C, 63.49 (56.09), H, 7.64 (6.17), N, 4.94 (4.88). FT-IR: 3752 cm^{-1} (O-H (alcohol), solvent), 2982 cm^{-1}, 2905 cm^{-1} (C-H (alkyl)), 1608 cm^{-1}, 1541 cm^{-1}, 1450 cm^{-1} (C=C (Ar), C=O (acetate)). Effective magnetic moment = 5.18 μ_B at 298 K in $CDCl_3$.

The elemental analysis of this complex is not optimal. This is presumably related to unreacted $Fe(OAc)_2$. It is reported here as the structure has been determined.

Fe(6$_{RR}$)OAc: Yield = 0.418 g, 80%. ESI-MS (MeCN): Calcd *m/z* $[C_{26}H_{34}FeN_2O_2]^+$ = 462.1970, found *m/z* = 462.2102. Elemental analysis: Calcd for $C_{30}H_{42.4}FeN_2O_{5.3}$ (From solid-state structure) (found): C, 63.03 (62.96), H, 7.48 (7.38), N, 4.90 (4.99). FT-IR: 2964 cm^{-1}, 2910 cm^{-1} (C-H (alkyl)), 1718 cm^{-1}, 1609 cm^{-1}, 1540 cm^{-1}, 1471 cm^{-1}, 1445 cm^{-1} (C=C (Ar), C=O (acetate)). Effective magnetic moment = 5.58 μ_B at 298 K in $CDCl_3$ (Based on solid-state structure).

Fe(6$_{SS}$)OAc: Yield = 0.423 g, 81%. ESI-MS (MeCN): Calcd *m/z* $[C_{26}H_{34}FeN_2O_2]^+$ = 462.1970, found *m/z* = 462.2123. Elemental analysis: Calcd for $C_{28}H_{37}FeN_2O_4$ (found): C, 64.49 (63.65), H, 7.15 (7.32), N, 5.37 (5.29). FT-IR: 2964 cm^{-1}, 2910 cm^{-1} (C-H (alkyl)), 1721 cm^{-1}, 1609 cm^{-1}, 1543 cm^{-1}, 1471 cm^{-1}, 1445 cm^{-1} (C=C (Ar), C=O (acetate)). Effective magnetic moment = 5.58 μ_B at 291 K in $CDCl_3$.

Fe(7)OAc: Yield = 0.510 g, 74%. ESI-MS (MeCN): Calcd *m/z* $[C_{38}H_{58}FeN_2O_2]^+$ = 630.3848, found *m/z* = 630.3863. Elemental analysis: Calcd for $C_{40}H_{61}FeN_2O_4$ (found): C, 69.65 (69.33), H, 8.91 (8.92), N, 4.06 (4.15). FT-IR: 2948 cm^{-1}, 2901 cm^{-1}, 2865 cm^{-1} (CH (alkyl)), 1519 cm^{-1}, 1390 cm^{-1}, 1469 cm^{-1}, 1440 cm^{-1}, 1411 cm^{-1} (C=C (Ar), C=O (acetate)). Effective magnetic moment = 5.58 μ_B at 298 K in $CDCl_3$.

Fe(8)OAc: Yield = 0.445 g, 67%. ESI-MS (MeCN): Calcd *m/z* $[C_{36}H_{56}FeN_2O_2]^+$ = 604.3691, found *m/z* = 604.3683. Elemental analysis: Calcd for $C_{38}H_{57}FeN_2O_4$ (found): C, 68.97 (67.99) H, 8.68 (9.10), N, 4.23 (4.29). FT-IR: 2947 cm^{-1}, 2905 cm^{-1}, 2866 cm^{-1} (CH (alkyl)), 1551 cm^{-1}, 1459 cm^{-1}, 1438 cm^{-1}, 1415 cm^{-1} (C=C (Ar), C=O (acetate)). Effective magnetic moment = 5.38 μ_B at 298 K in $CDCl_3$.

Fe(9)OAc: Yield = 0.091 g, 24%. ESI-MS (MeCN): Calcd *m/z* $[C_{16}H_{14}FeN_2O_2]^+$ = 322.0405, found *m/z* = 322.0424. Elemental analysis: Calcd for $C_{18}H_{17}FeN_2O_4$ (found): C, 56.72 (52.46) H, 4.50 (4.02), N, 7.35 (7.37). FT-IR: 3671 cm^{-1} (O-H (alcohol), solvent), 2988 cm^{-1}, 2970 cm^{-1}, 2901 cm^{-1} (C-H (alkyl)), 1626 cm^{-1} (C=N), 1597 cm^{-1}, 1539 cm^{-1}, 1466 cm^{1} (C=C (Ar), C=O (acetate)). Effective magnetic moment = 3.29 μ_B at 298 K in $CDCl_3$.

The elemental analysis results are more in with Fe(**9**)OAc·H_2O, potentially indicative of the hygroscopic nature of the complex.

Fe(10)OAc: Yield = 0.091 g, 15%. ESI-MS (MeCN): Calcd *m/z* $[C_{32}H_{46}FeN_2O_2]^+$ = 546.2909, found *m/z* = 546.3028. Elemental analysis: Calcd for $C_{34}H_{49}FeN_2O_4$ (found): C, 67.43 (64.46), H, 8.16 (7.89), N, 4.63 (4.64). FT-IR: 2954 cm^{-1}, 2923 cm^{-1}, 2903 cm^{-1}, 2868 cm^{-1} (C-H (alkyl)), 1621 cm^{-1} (C=N), 1546 cm^{-1}, 1535 cm^{-1}, 1457 cm^{-1}, 1437 cm^{-1}, 1411 cm^{1} (C=C (Ar), C=O (acetate)). Effective magnetic moment = 4.61 μ_B at 298 K in $CDCl_3$.

The elemental analysis results are more in with Fe(**10**)OAc·H_2O, potentially indicative of the hygroscopic nature of the complex.

Fe(11)OAc: Yield = 0.308 g, 72%. ESI-MS (MeCN): Calcd *m/z* $[C_{20}H_{14}FeN_2O_2]^+$ = 370.0405, found *m/z* = 370.0550. Elemental analysis: Calcd for $C_{38}H_{49}FeN_2O_4$ (found): C, 61.56 (61.08), H, 3.99 (3.98), N, 6.53 (6.62). FT-IR: 3661 cm^{-1} (O-H (alcohol), solvent), 2971 cm^{-1} (C-H (alkyl)), 1610 cm^{-1} (C=N), 1578 cm^{-1}, 1529 cm^{-1}, 1463 cm^{-1}, 1434 cm^{-1} (C=C (Ar), C=O (acetate)). Effective magnetic moment = 4.66 μ_B at 290 K in $CDCl_3$.

Fe(12)OAc: Yield = 0.313 g, 48%. ESI-MS (MeCN): Calcd *m/z* $[C_{36}H_{46}FeN_2O_2]^+$ = 594.2909, found *m/z* = 594.2919. Elemental analysis: Calcd for $C_{38}H_{49}FeN_2O_4$ (found): C, 69.82 (71.74), H, 7.56 (7.84), N, 4.29 (4.80). FT-IR: 2952 cm^{-1}, 2905 cm^{-1}, 2869 cm^{-1} (CH (alkyl)), 1601 cm^{-1} (C=N), 1580 cm^{-1}, 1551 cm^{-1}, 1527 cm^{-1}, 1457 cm^{-1}, 1425 cm^{-1}, 1412 cm^{-1} (C=C (Ar), C=O (acetate)). Effective magnetic moment = 2.01 μ_B at 298 K in $CDCl_3$.

General CO_2 / epoxide coupling reaction method and procedure

All CO_2 / epoxide coupling reactions were carried out in a ratio of 1:8:1200 [catalyst (0.08 mol%)]:[co-catalyst (0.64 mol%)]:[epoxide] where generally tetrabutylammonium chloride (TBAC) was the co-catalyst and cyclohexene (CHO) was the epoxide.

The catalyst (4.21 x 10^{-5} mol) and TBAC (0.094 g, 3.37 x 10^{-4} mol) were added as solids to a glass reactor vial in a glovebox. CHO (5 mL) was added to the vial *via* syringe to form a dark purple mixture. The vial was transferred out of the glovebox and placed in the autoclave under a flow of argon. The autoclave was cycled five times with CO_2 and finally left pressurised at 10 bar. The temperature was ramped to 80 °C and left for 24 hours with mechanical stirring. After this time, the autoclave was cooled in an ice bath before bleeding to the air. An aliquot was taken of the crude dark red product mixture and analysed *via* ^{1}H NMR spectroscopy to determine conversion and selectivity. Electrospray ionisation-mass spectrometry (ESI-MS) was used to confirm the cyclic carbonate product was present in the mixture and gel permeation chromatography (GPC) analysis to confirm no polymer was present.

Crude ^{1}H NMR spectra of CO_2 / epoxide coupling reaction mixtures

Table 2. *Entry 6*, Epoxide = Cyclohexene oxide (CHO)

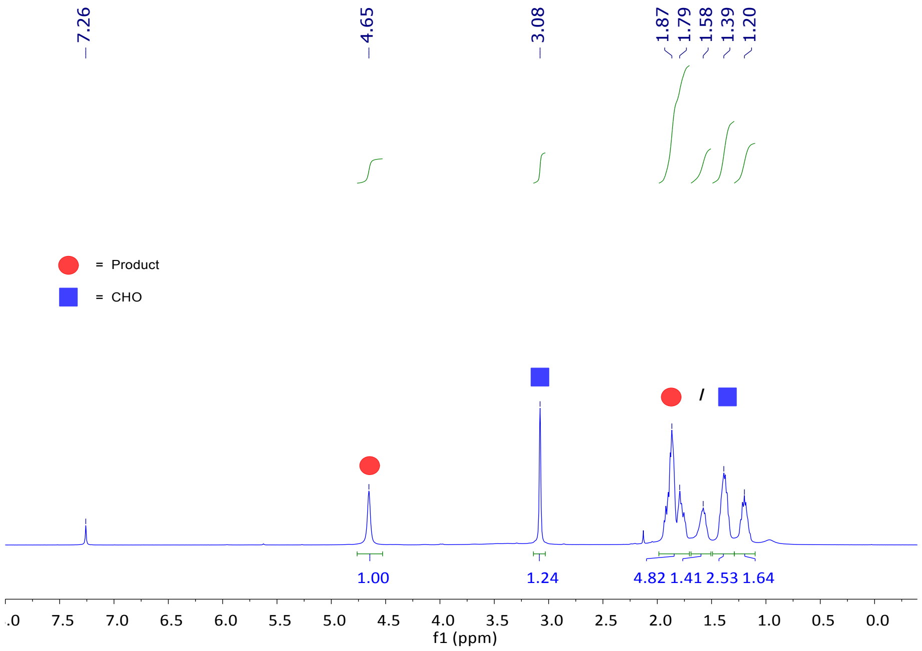

^{1}H NMR spectroscopy consistent with literature.[5–7] ESI-MS (MeCN): Calcd *m/z* $[C_7H_{11}O_3]^+$ = 143.0703, found *m/z* = 143.0729, calcd *m/z* $[C_7H_{10}O_3Na]^+$ = 165.0522, found *m/z* = 165.0553.

Table 2. *Entry 19*, Epoxide = Cyclohexene oxide (CHO)

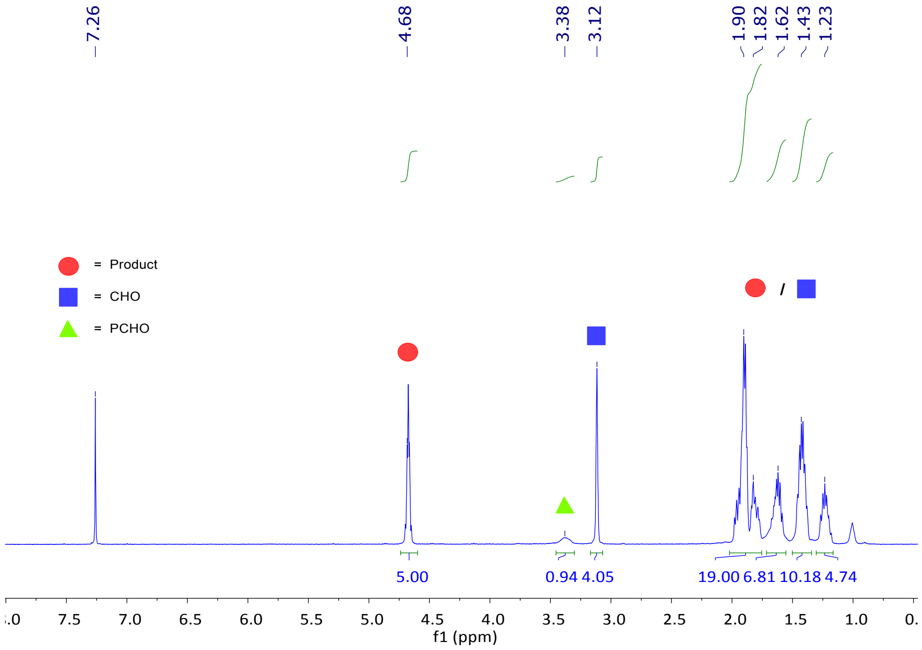

Table 4. *Entry 1*, Epoxide = Propylene oxide (PO)

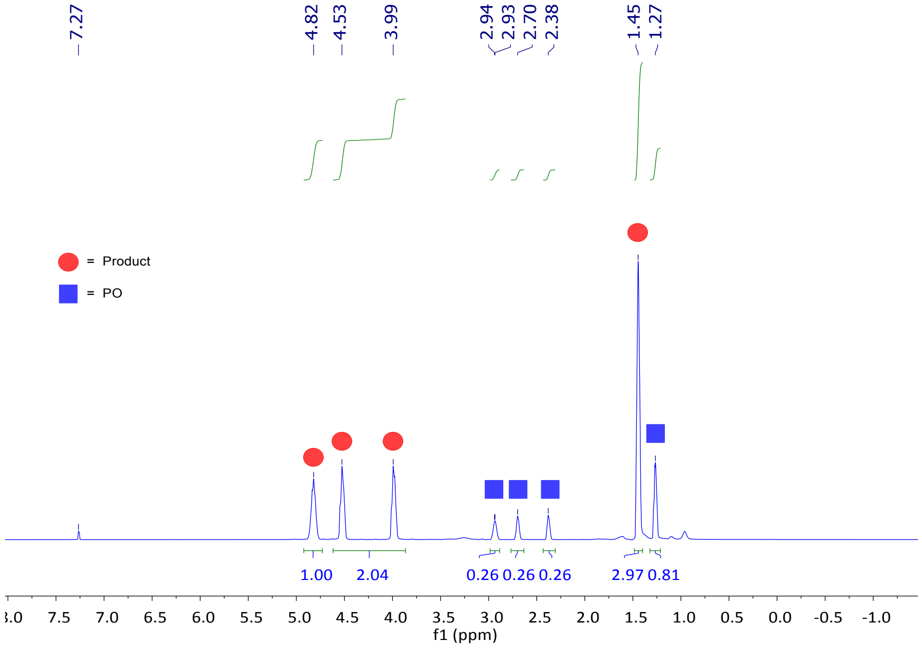

^{1}H NMR spectroscopy consistent with literature.[5–7] ESI-MS (MeCN): Calcd *m/z* $[C_4H_7O_3]^+$ = 103.0390, found *m/z* = 103.0393, calcd *m/z* $[C_4H_6O_3Na]^+$ = 125.0209, found *m/z* = 125.0223.

Table 4. *Entry 2*, Epoxide = Styrene oxide (SO)

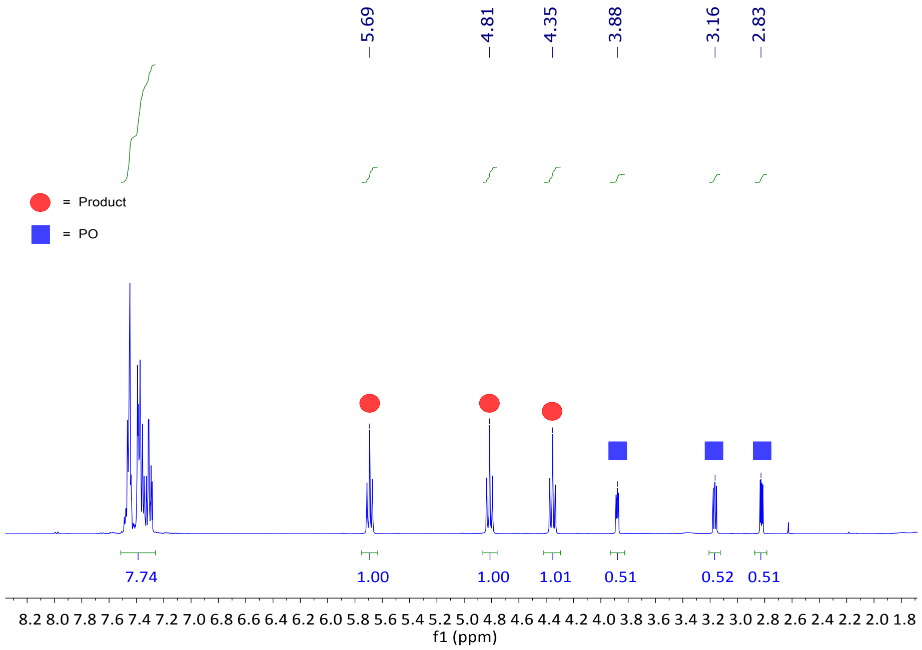

^{1}H NMR spectroscopy consistent with literature.[5–7] ESI-MS (MeCN): Calcd *m/z* $[C_9H_9O_3]^+$ = 165.0546, found *m/z* = 165.0588, calcd *m/z* $[C_9H_8O_3Na]^+$ = 187.0366, found *m/z* = 187.0391.

Table 4. *Entry 3*, Epoxide = Epichlorohydrin (ECH)

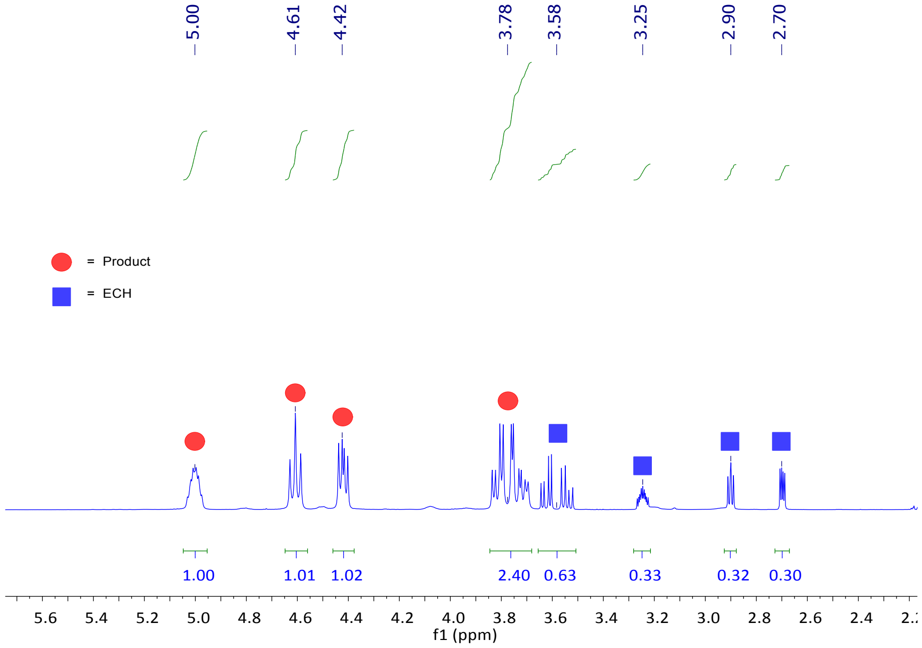

^{1}H NMR spectroscopy consistent with literature.[5–7]

Table 4. *Entry 4*, Epoxide = Phenyl glycidyl ether (PGE)

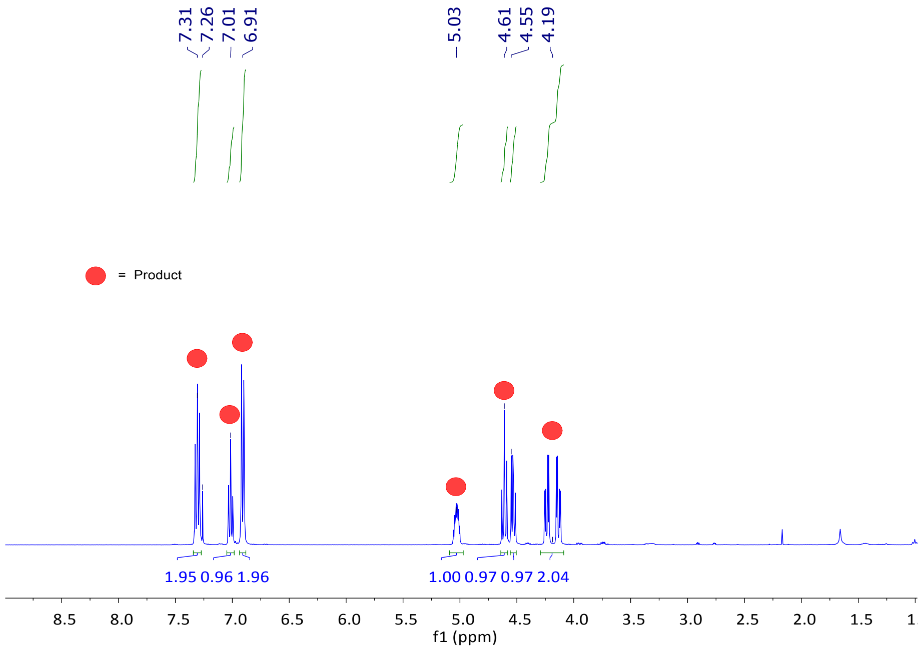

^{1}H NMR spectroscopy consistent with literature.[5,6] ESI-MS (MeCN): Calcd *m/z* $[C_{10}H_{11}O_4]^+$ = 195.0652, found *m/z* = 195.0596, calcd *m/z* $[C_{10}H_{10}O_4Na]^+$ = 217.0471, found *m/z* = 217.0405.

Table 4. *Entry 6*, Epoxide = Allyl glycidyl ether (AGE)

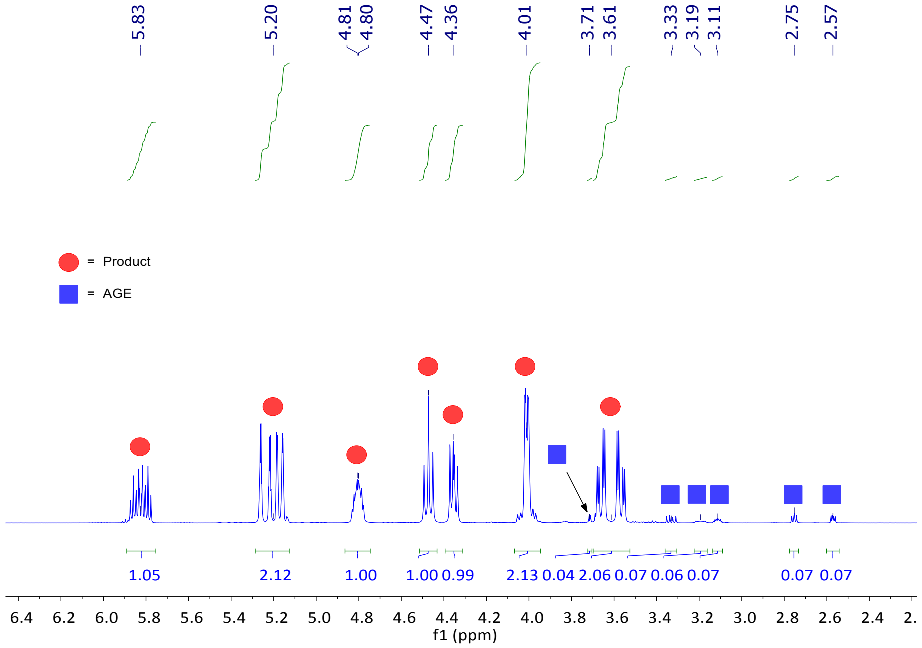

^{1}H NMR spectroscopy consistent with literature.[6,7] ESI-MS (MeCN): Calcd *m/z* $[C_7H_{11}O_4]^+$ = 159.0652, found *m/z* = 159.0703, calcd *m/z* $[C_7H_{10}O_4Na]^+$ = 181.0471, found *m/z* = 181.0491.

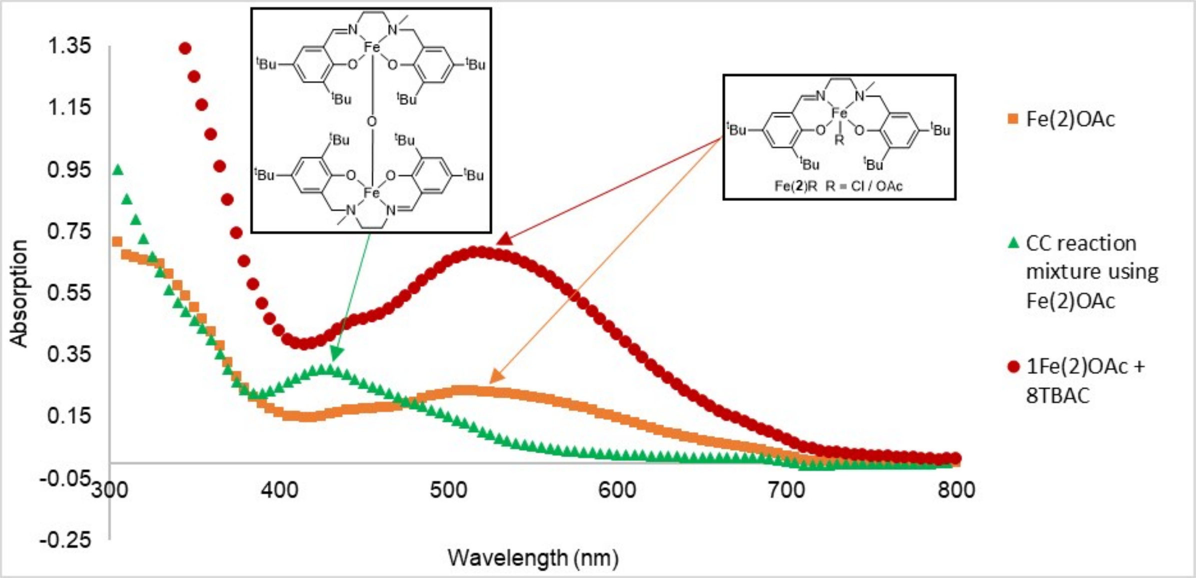

Figure 1: UV-Vis spectra of Fe(**2**)OAc, Fe(**2**)OAc in the presence of 8 eq. TBAC and the crude reaction mixture using Fe(**2**)OAc.

General polymerisation methods and procedures

All polymerisations were carried out using Schlenk flasks with J Youngs taps under inert conditions. Polymerisations were generally carried out in a ratio of 100:1:1:1 [LA]:[Fe]:[BnOH]:[NEt_3].

Solution polymerisation

Fe(**X**)OAc (0.028 mmol) and *rac*-lactide (0.40 g, 2.80 mmol) were placed in a flask and dry toluene (4 mL) and triethylamine (0.028 mmol) and benzyl alcohol (0.028 mmol) were added. The overall loading was 100:1:1:1 [LA]:[Fe]:[Et_3N]:[BnOH]. The flask was placed in the pre-heated oil bath (100 °C / 80 °C) for 24 hours. After this reaction time, the flask was cooled and dichloromethane (DCM) was added to dissolve the polymer and transfer all contents into a round bottom flask. The solvent was removed *in vacuo* and further dried before being analysed by ^{1}H NMR Spectroscopy ($CDCl_3$) to determine conversion to polymer. The residue was washed with excess methanol (>30 mL) to remove any impurities and dried before being analysed by ^{1}H{^{1}H} NMR spectroscopy ($CDCl_3$), GPC and MALDI-ToF.

All washed polymers were characterised by gel permeation chromatography (GPC). GPC was carried out at 1 ml min^{-1} at 35 °C with a THF eluent using a PLgel 5 µm MIXED-D 300 × 7.5 mm column. Molecular weights were determined using refractive index (RI). Homonuclear decoupled NMR spectroscopy, ^{1}H {^{1}H}, was used to determine the probability of isotactic enchainment, P_m.[8] MALDI-ToF mass spectra were determined on a Bruker Autoflex speed instrument using DCTB {trans-2-[3-(4-tert-Butylphenyl)-2-methyl-2-propenylidene]malononitrile} as the matrix and ionized using NaTFA. Spectra were recorded in positive reflectron mode.

Materials characterisation (GPC, ESI-MS MALDI-TOF) facilities were provided through the Chemical Characterisation and Analysis Facility (CCAF) at the University of Bath.

Polymer Characterisation

Homonuclear decoupled spectra

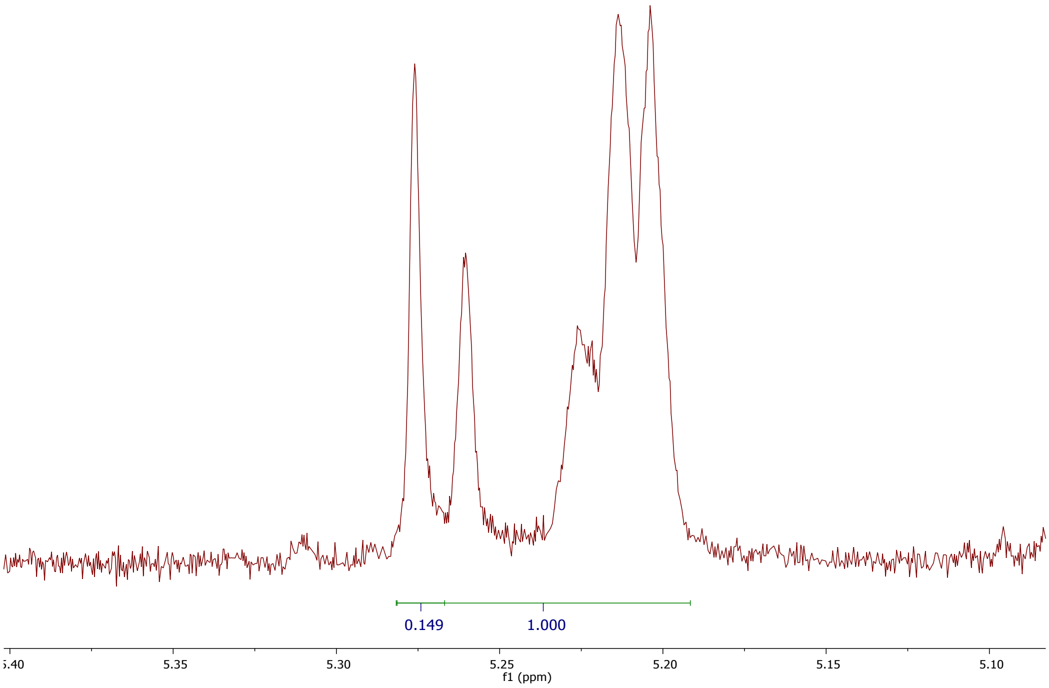

Figure 2: $^{1}H\{^{1}H\}$ NMR spectra of polymer prepared with Fe(**3**)OAc (100°C; P_m = 0.45).

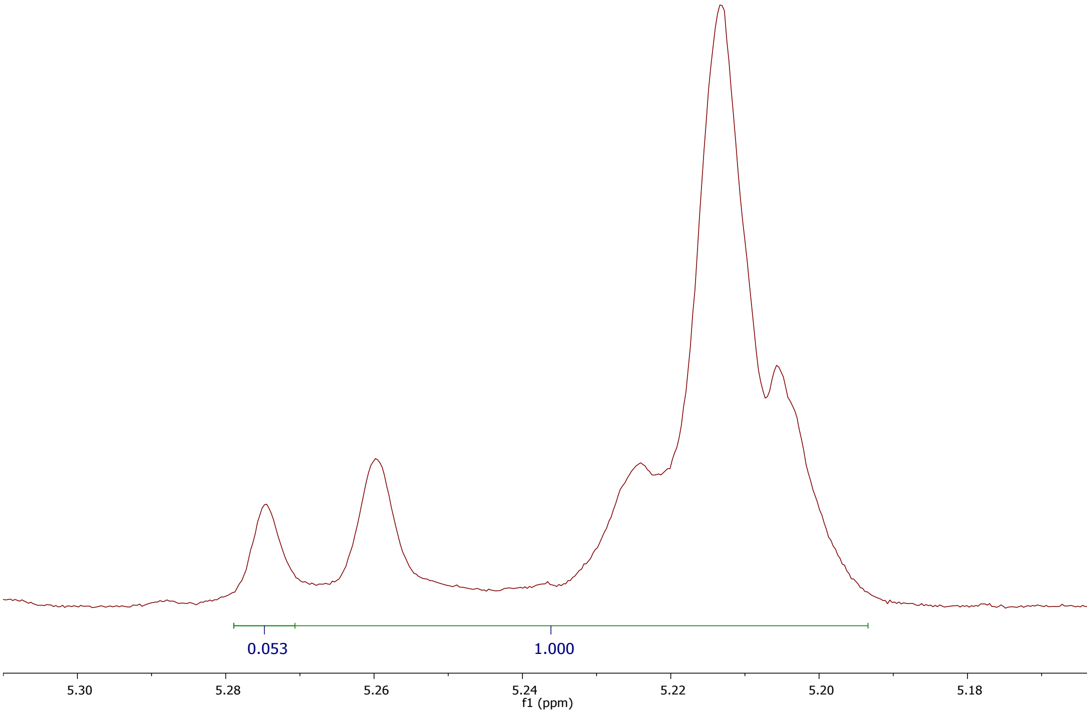

Figure 3: $^{1}H\{^{1}H\}$ NMR spectra of polymer prepared with Fe(**8**)OAc (100°C; P_m = 0.67).

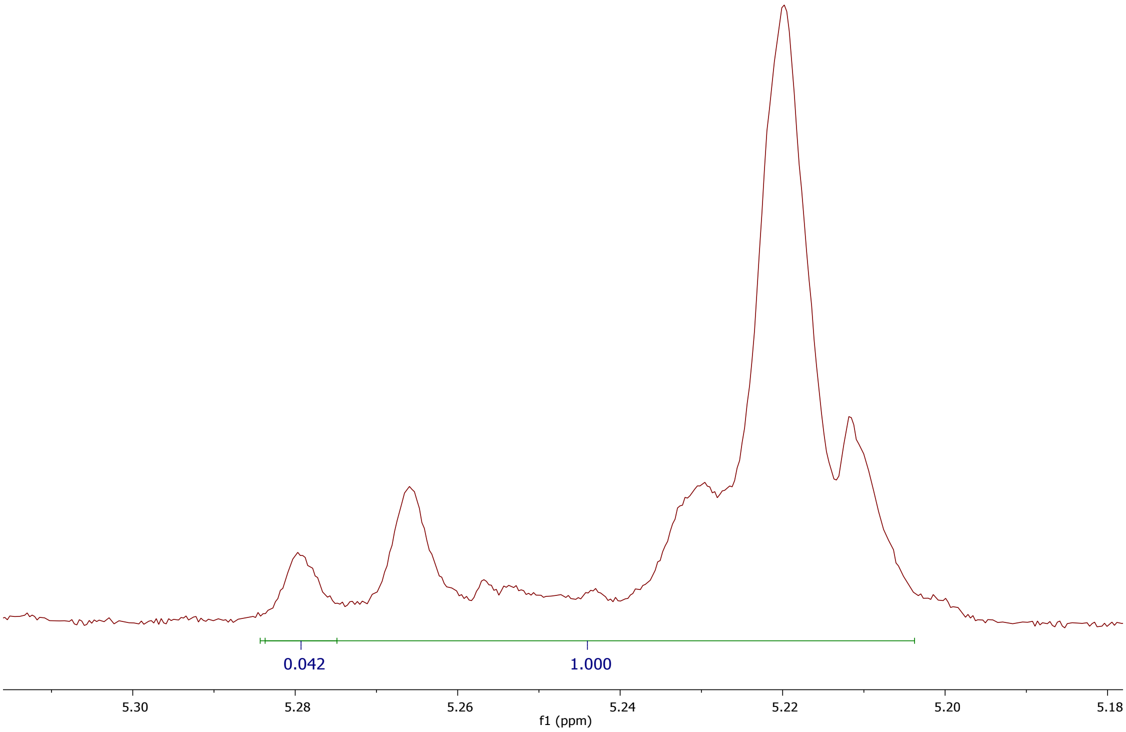

Figure 4: $^1H\{^1H\}$ NMR spectra of polymer prepared with Fe(**10**)OAc (100°C; P_m = 0.71).

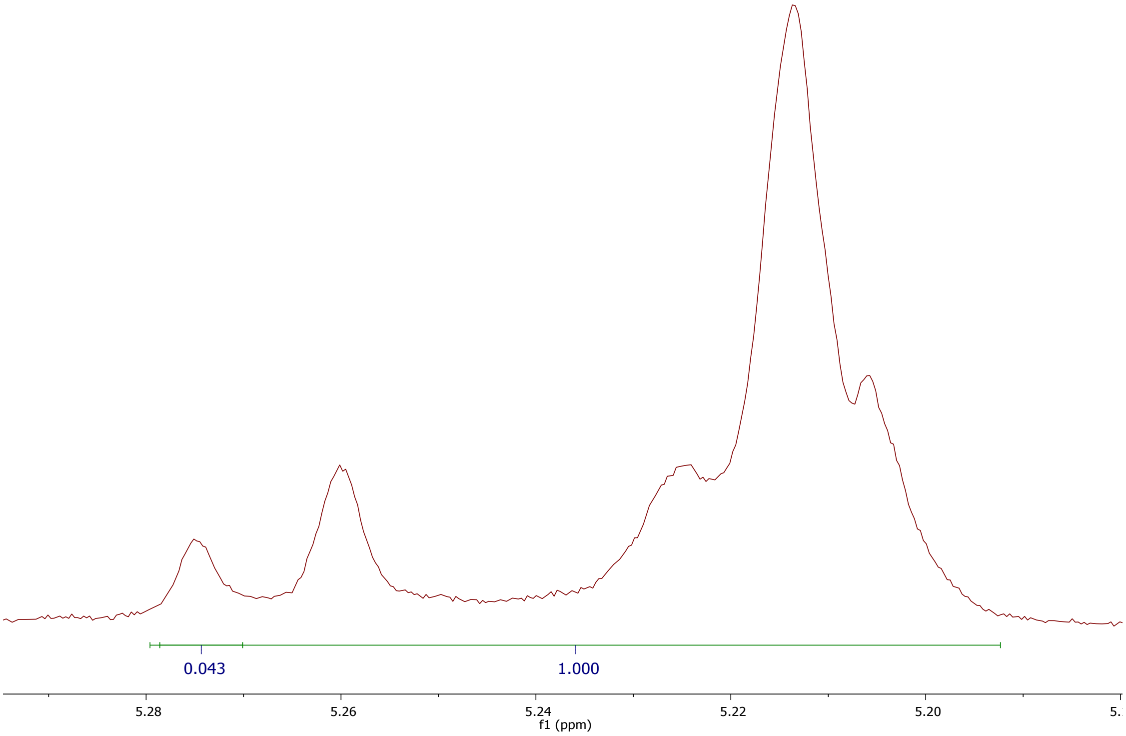

Figure 5: $^1H\{^1H\}$ NMR spectra of polymer prepared with Fe(**12**)OAc (100°C; P_m = 0.71).

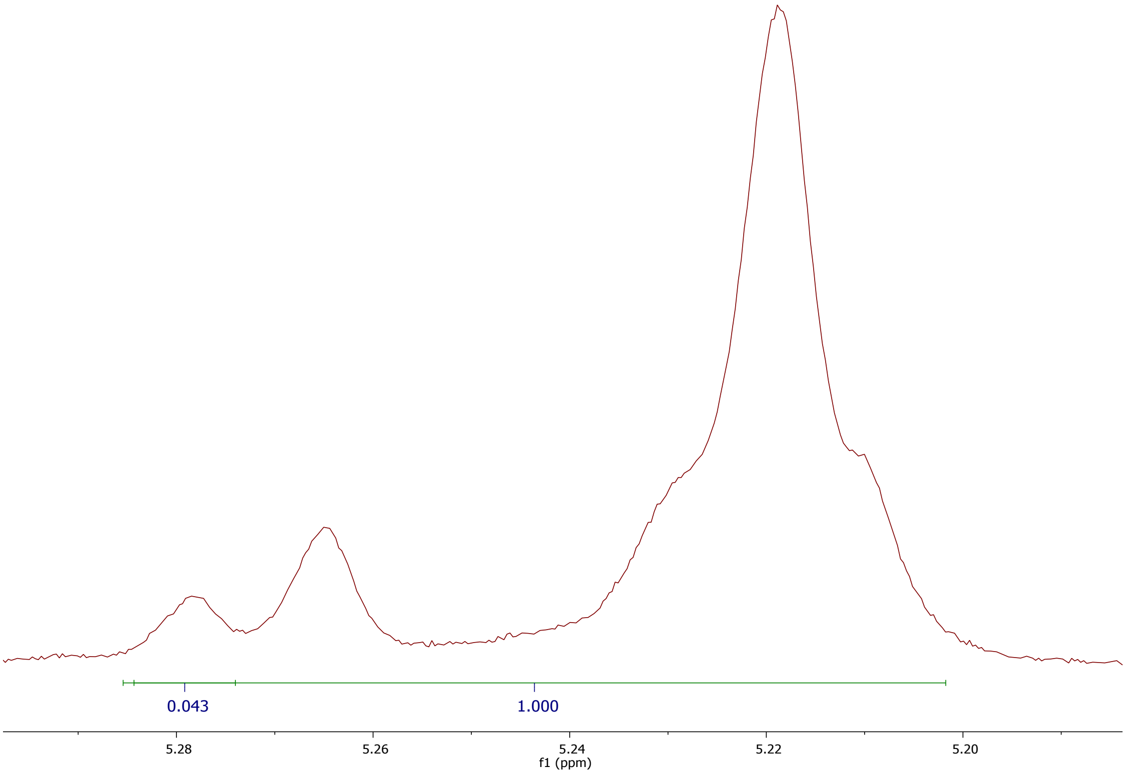

Figure 6: $^1H\{^1H\}$ NMR spectra of polymer prepared with Fe(**12**)OAc (80°C; $P_m = 0.71$).

GPC spectra

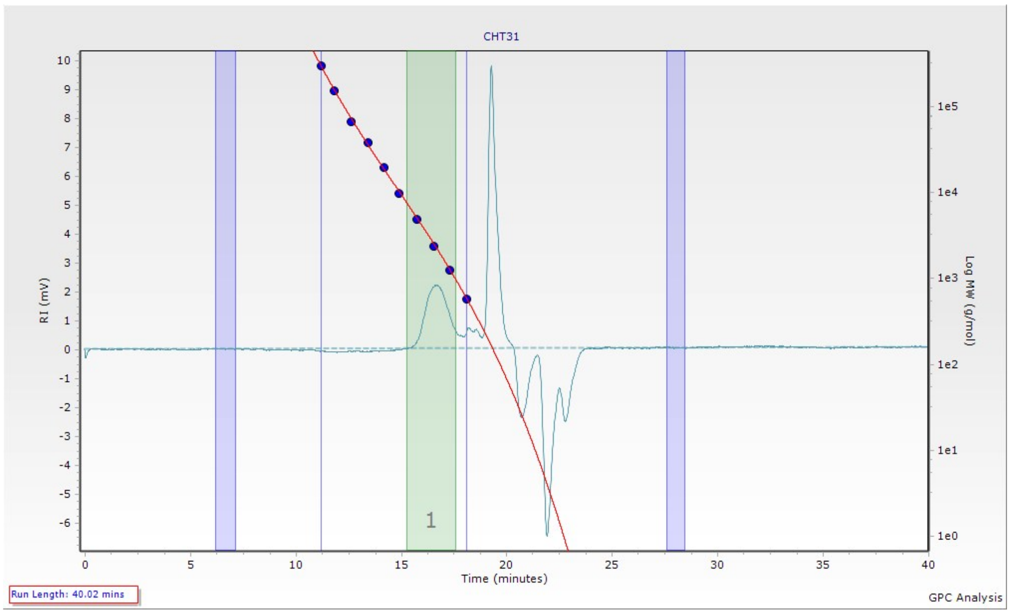

Figure 7: GPC chromatogram of polymer prepared with Fe(**1**)OAc (100°C; M_n = 2000 g mol^{-1}, Đ = 1.17; Table 6).

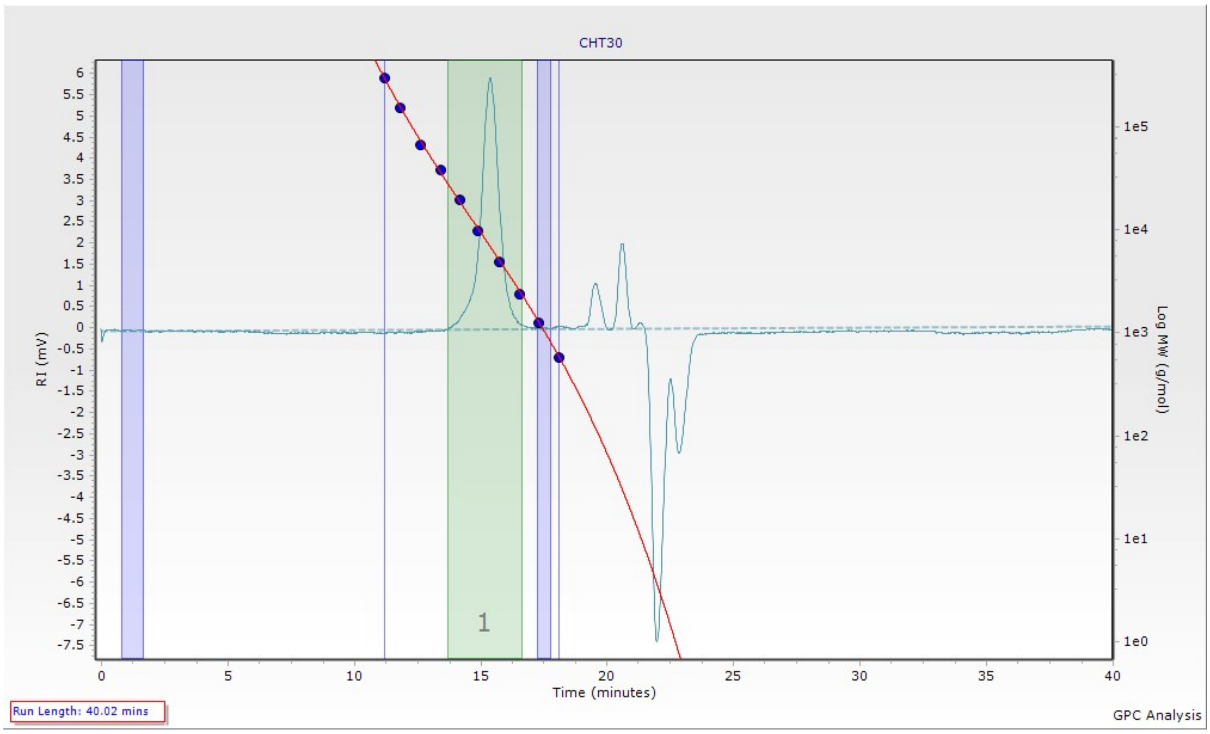

Figure 8: GPC chromatogram of polymer prepared with Fe(**2**)OAc (100°C; M_n = 6550 g mol^{-1}, Đ = 1.13; Table 6).

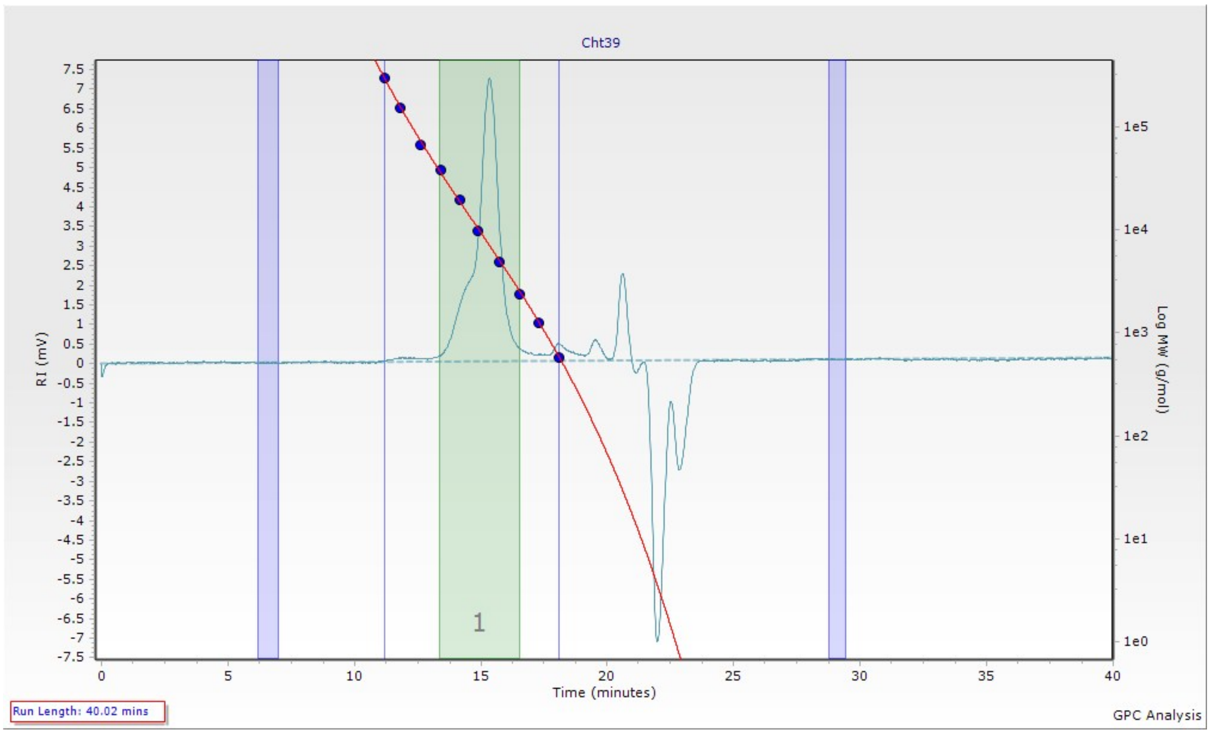

Figure 9: GPC chromatogram of polymer prepared with Fe(**3**)OAc (100°C; M_n = 7300 g mol^{-1}, Đ = 1.26; Table 6).

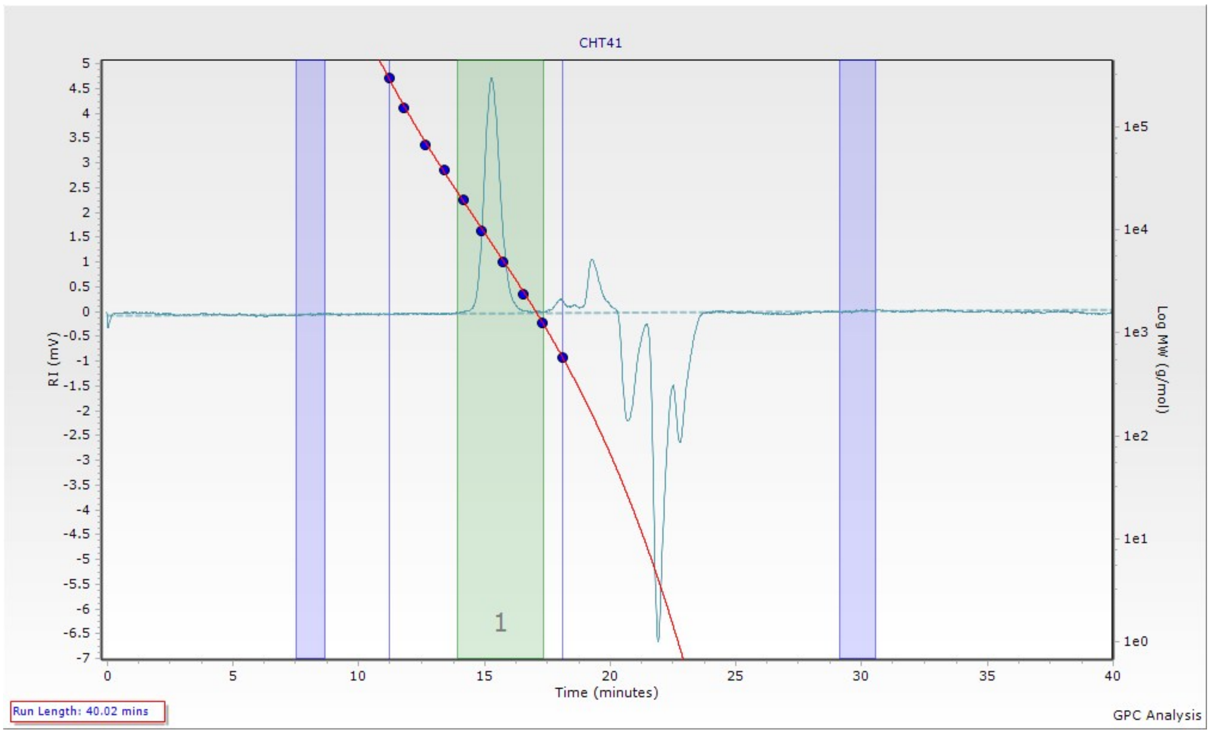

Figure 10: GPC chromatogram of polymer prepared with Fe(**5**)OAc (100°C; M_n = 6700 g mol^{-1}, Đ = 1.10; Table 6).

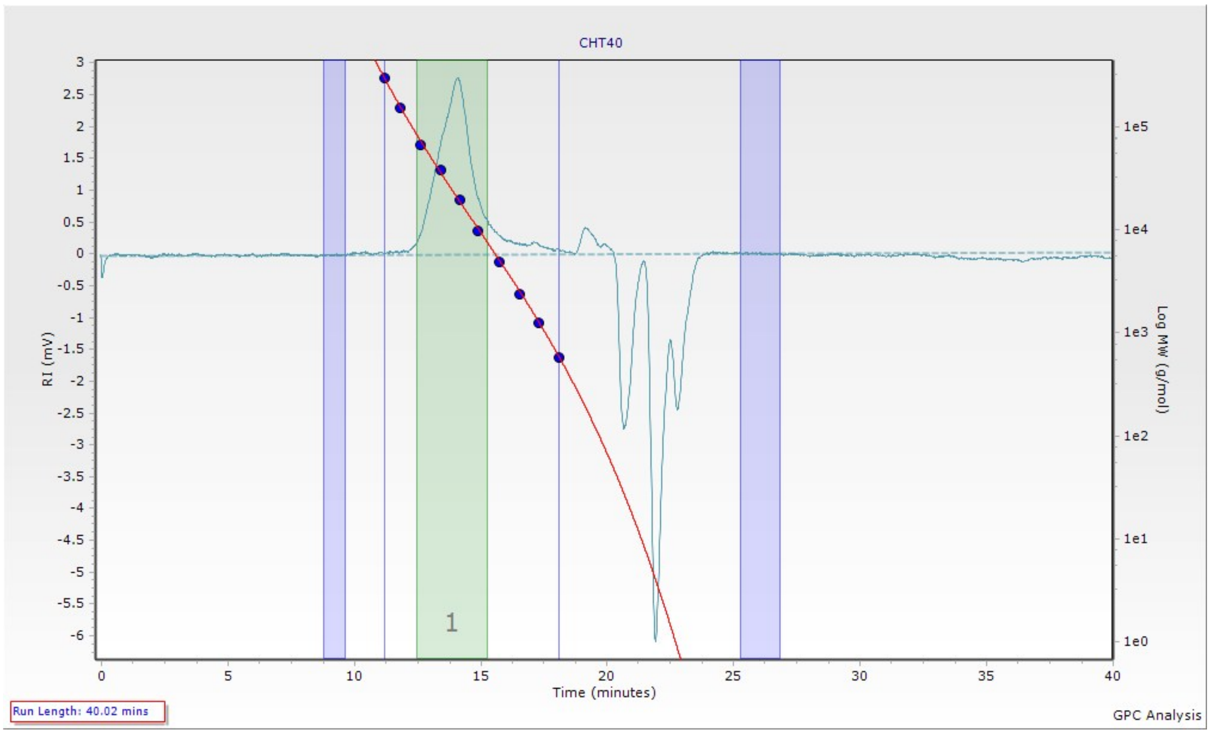

Figure 11: GPC chromatogram of polymer prepared with Fe(**6**$_{meso}$)OAc (100°C; M_n = 19900 g mol^{-1}, Đ = 1.30; Table 6).

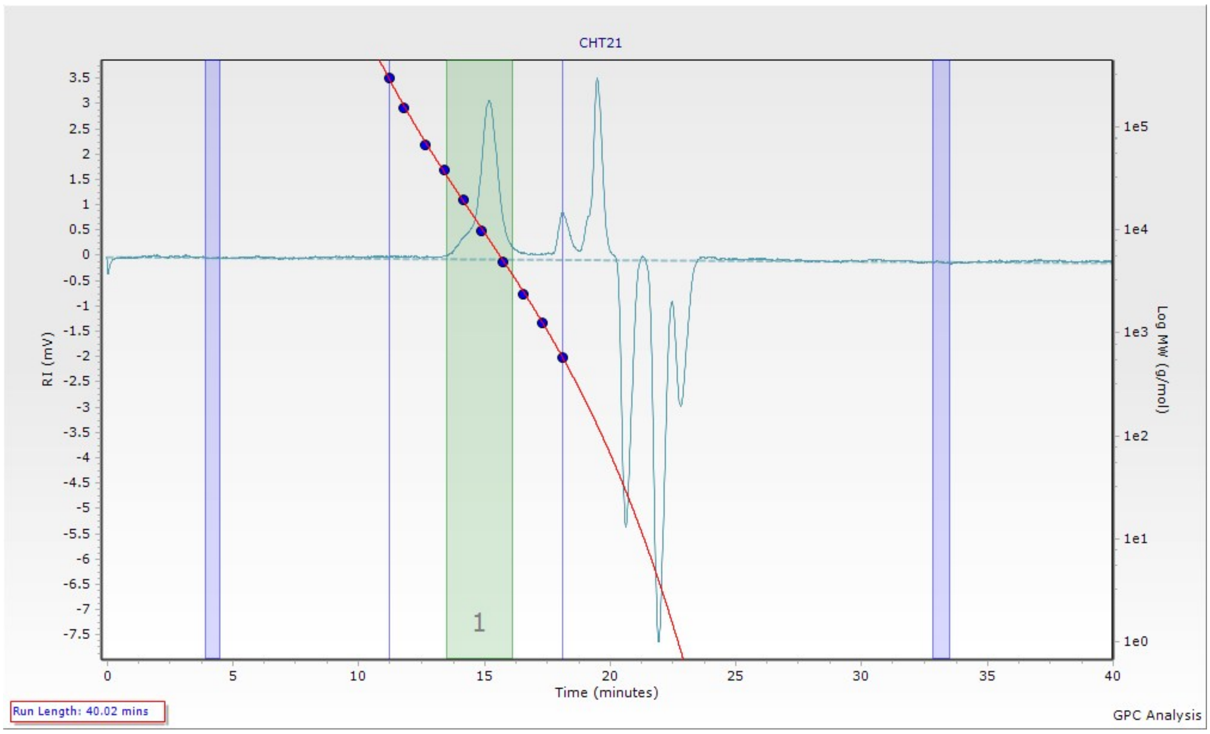

Figure 12: GPC chromatogram of polymer prepared with Fe(**7**)OAc (100°C; M_n = 6600 g mol^{-1}, Đ = 1.09; Table 6).

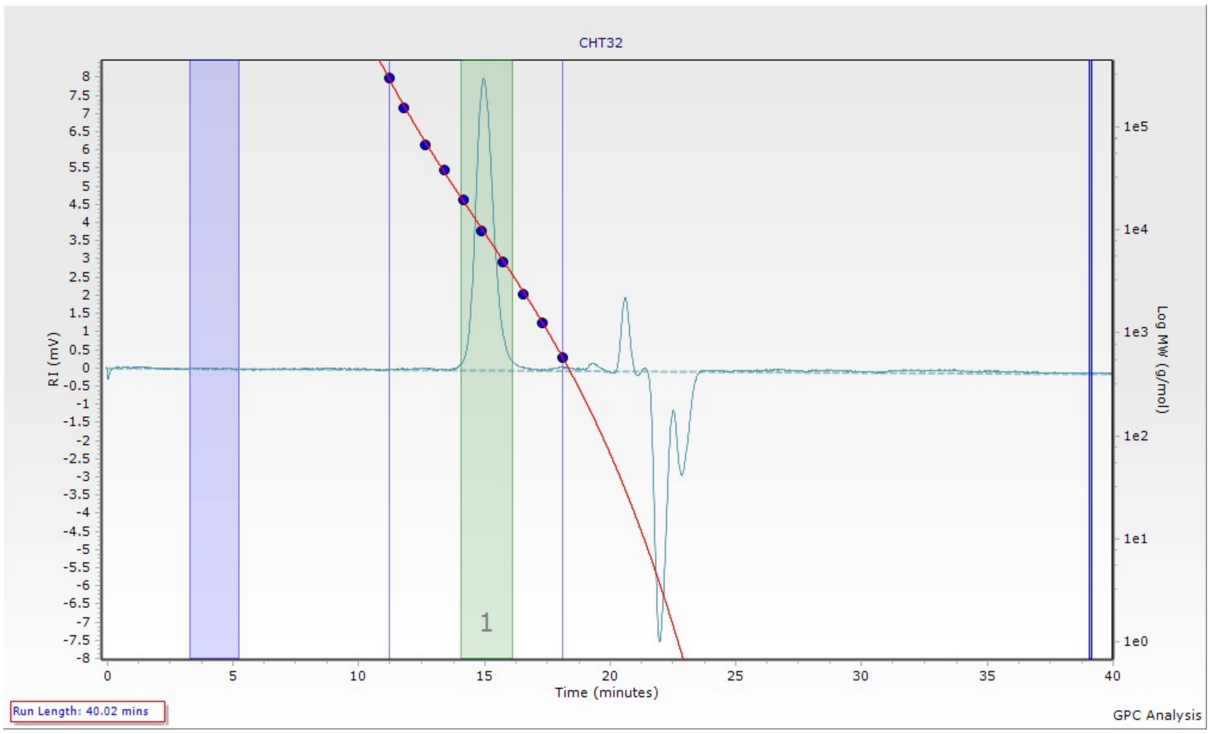

Figure 13: GPC chromatogram of polymer prepared with Fe(**8**)OAc (100°C; M_n = 8700 g mol^{-1}, Đ = 1.09; Table 6).

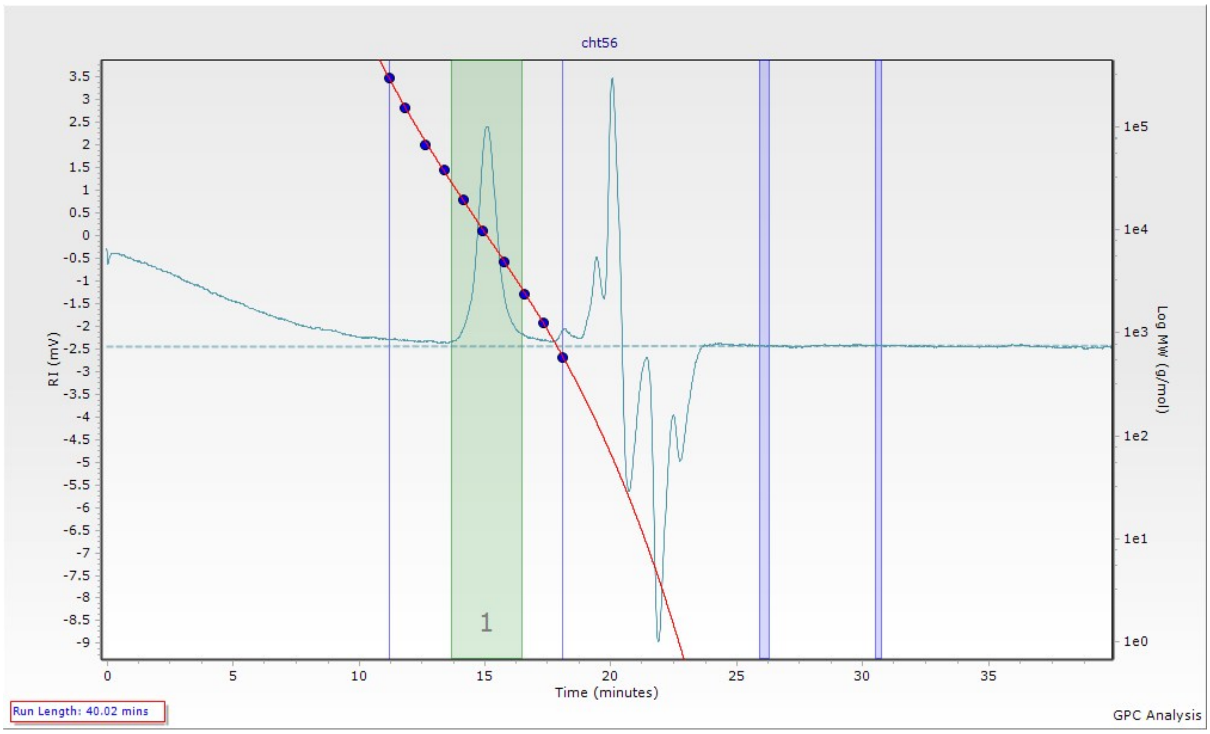

Figure 14: GPC chromatogram of polymer prepared with Fe(**10**)OAc (100°C; M_n = 7750 g mol^{-1}, Đ = 1.16; Table 6).

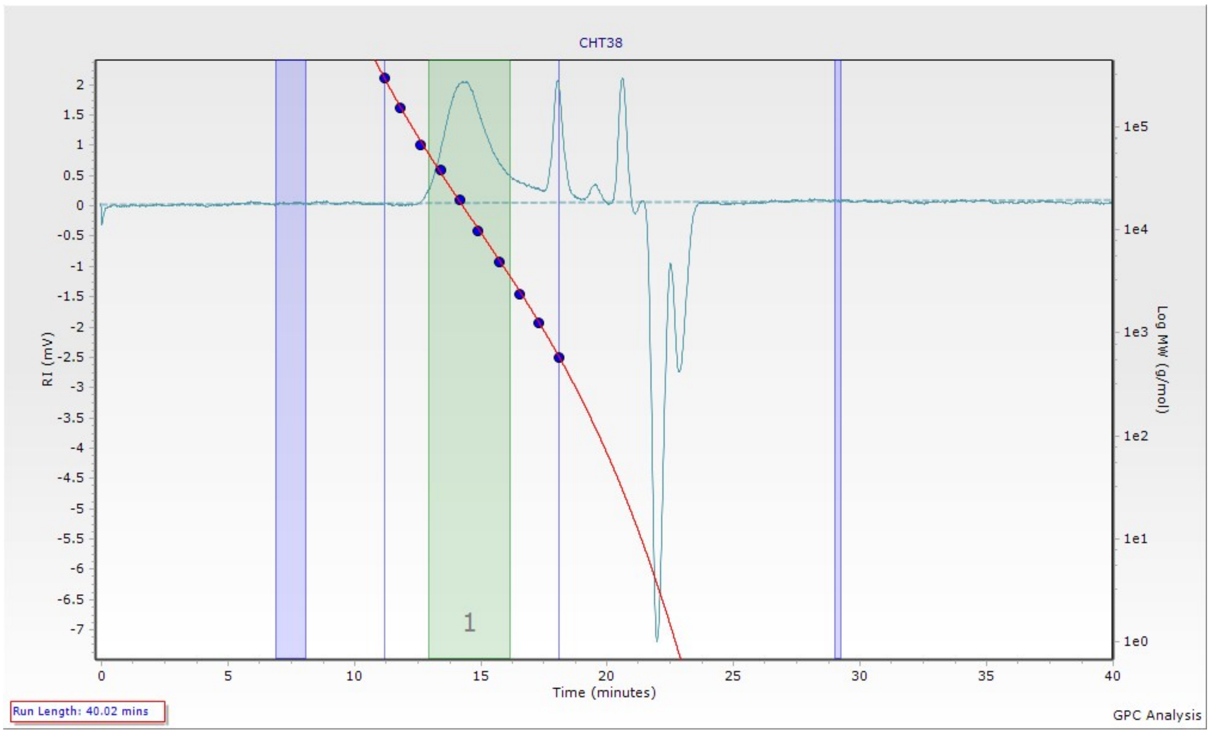

Figure 15: GPC chromatogram of polymer prepared with Fe(**12**)OAc (100°C; M_n = 11700 g mol^{-1}, Đ = 1.46; Table 6).

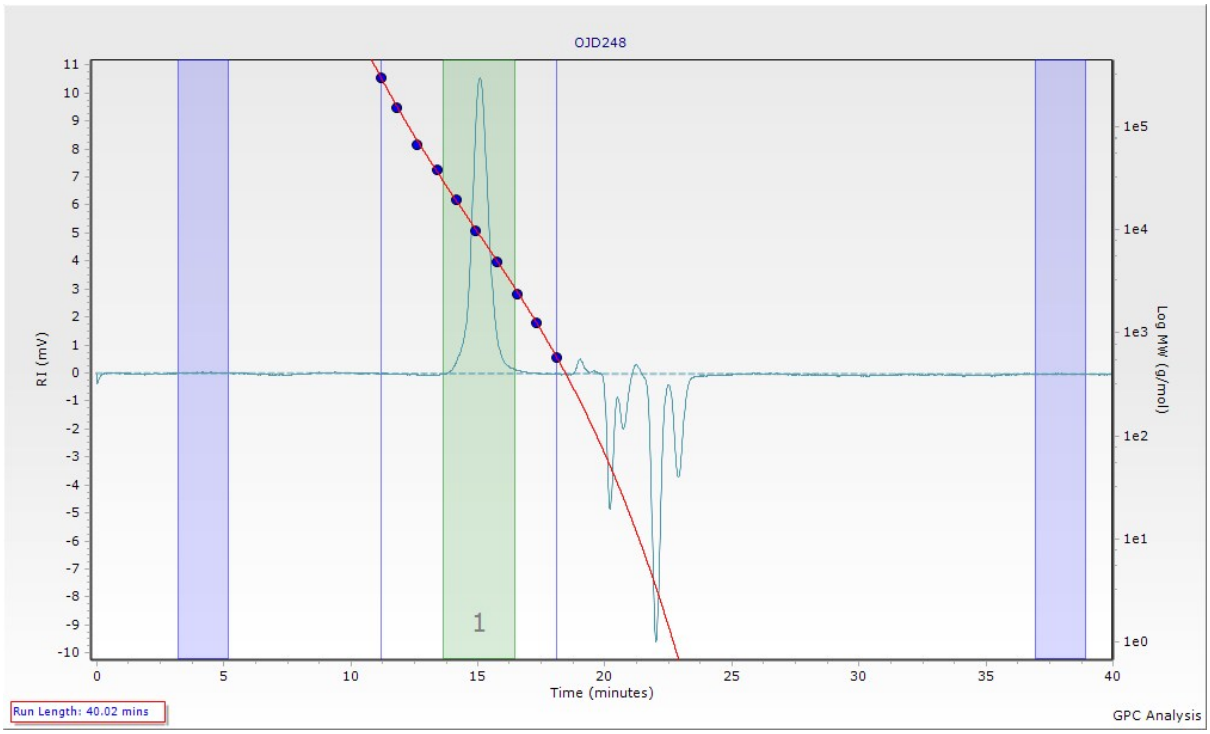

Figure 16: GPC chromatogram of polymer prepared with Fe(**6** $_{\textbf{\textit{meso}}}$)OAc (80°C; M_n = 8100 g mol^{-1}, Đ = 1.09; Table 7).

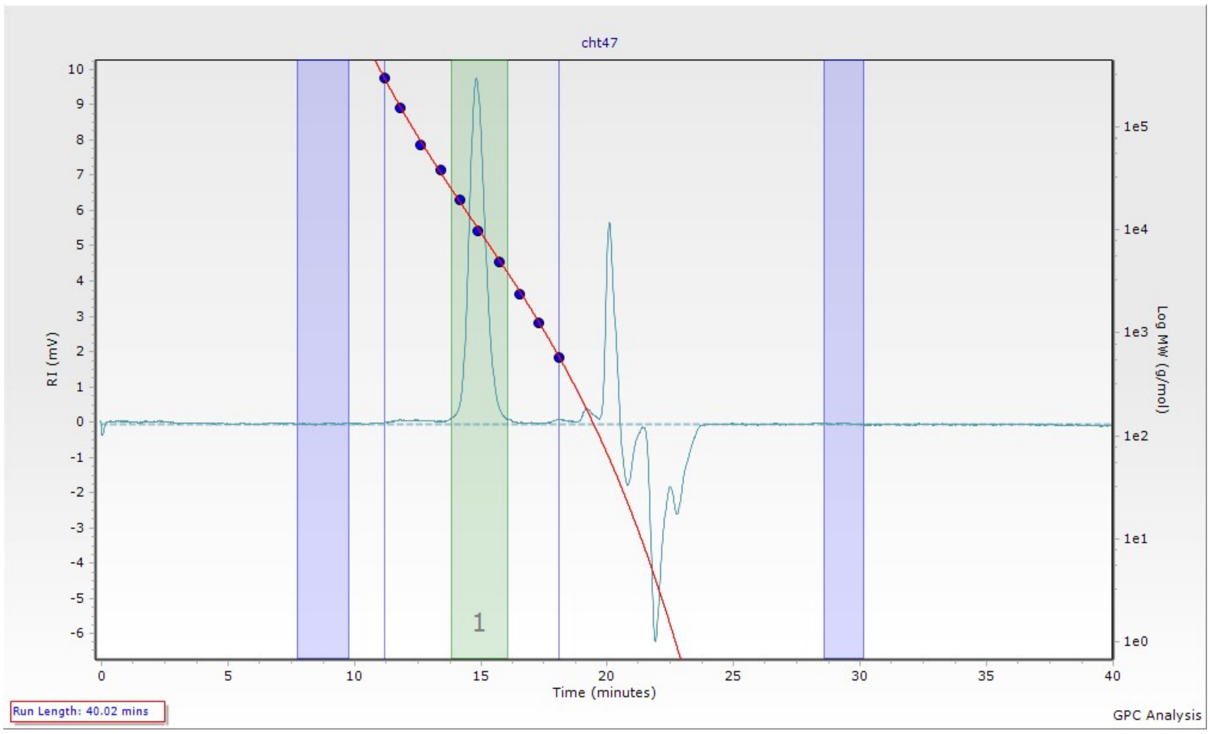

Figure 17: GPC chromatogram of polymer prepared with Fe(**8**)OAc (80°C; M_n = 9900 g mol^{-1}, Đ = 1.07; Table 7).

MALDI-ToF spectra

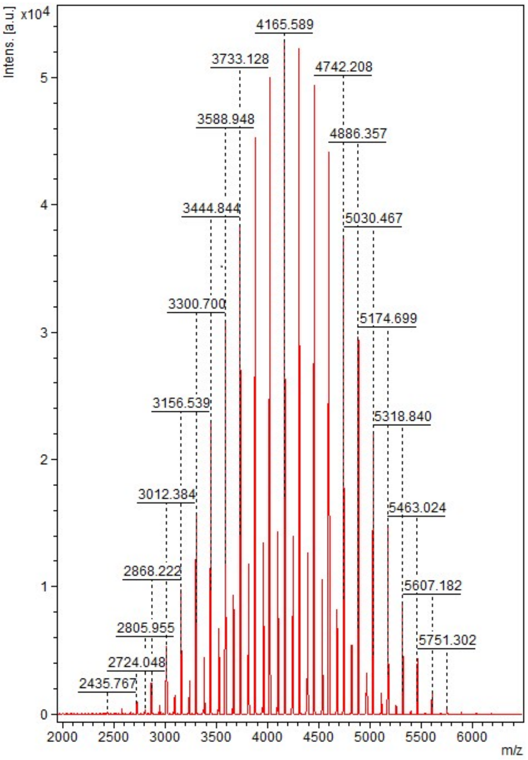

Figure 18: MALDI-ToF spectra of polymer prepared with Fe(**2**)OAc (100°C; M_n = 6550 g mol^{-1}, Đ = 1.13; Table 6).

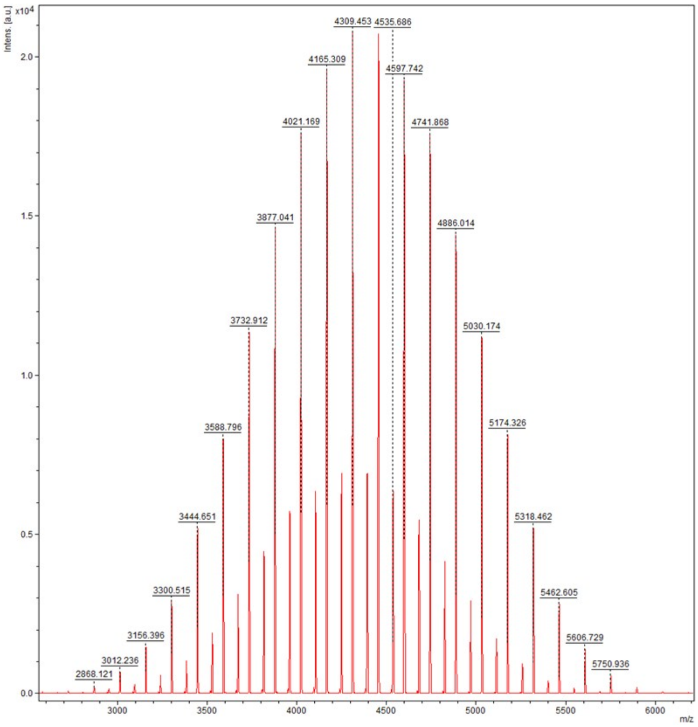

Figure 19: MALDI-ToF spectra of polymer prepared with Fe(**3**)OAc (100°C; M_n = 7300 g mol^{-1}, Đ = 1.26; Table 6).

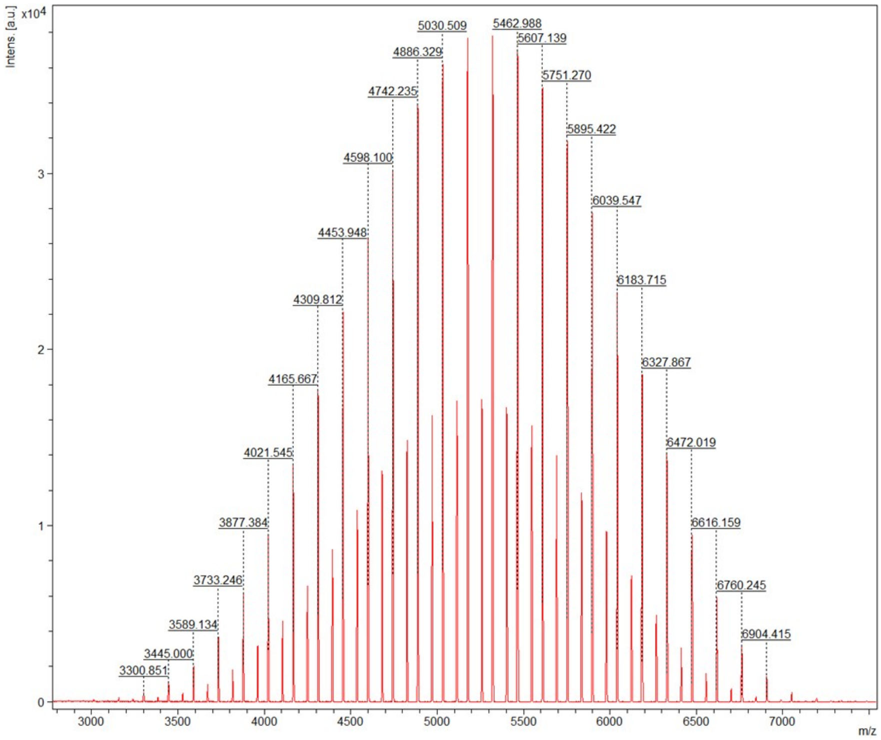

Figure 20: MALDI-ToF spectra of polymer prepared with Fe(**8**)OAc (100°C; M_n = 8700 g mol^{-1}, Đ = 1.09; Table 6).

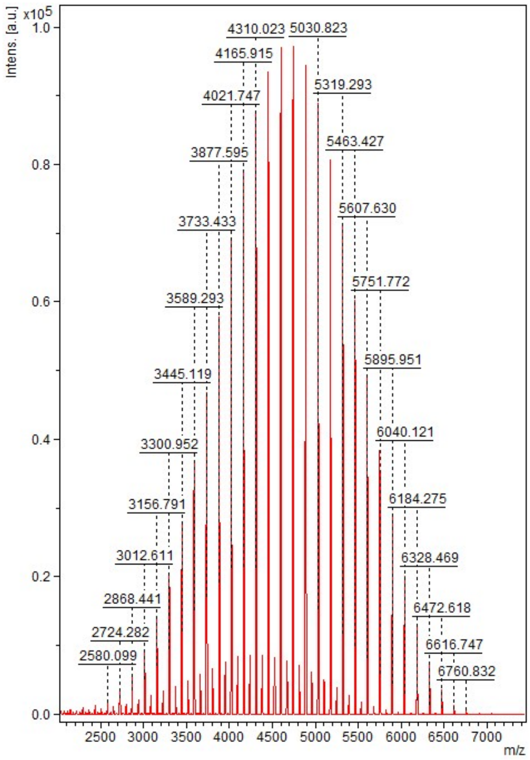

Figure 21: MALDI-ToF spectra of polymer prepared with Fe(**10**)OAc (100°C; M_n = 7750 g mol^{-1}, Đ = 1.16; Table 6).

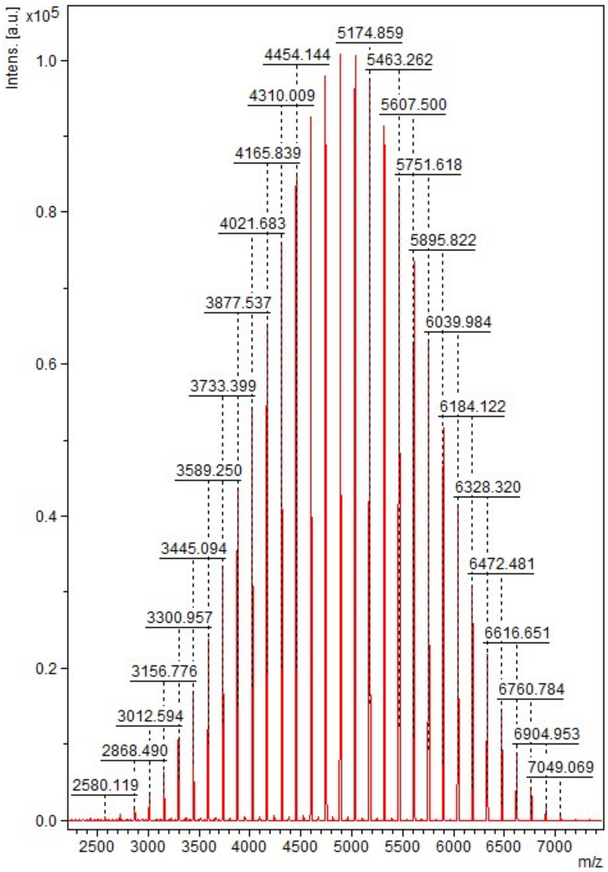

Figure 22: MALDI-ToF spectra of polymer prepared with Fe($\mathbf{6}_{\mathit{meso}}$)OAc (80°C; M_n = 8100 g mol^{-1}, Đ = 1.09; Table 7).

Table 1: Summary of MALDI-ToF data

	Series 1			Series 2	
Complex	M_p / g mol^{-1}	M_n	End Group	M_n / g mol^{-1}	End Group
Fe(**2**)OAc (100°C)	4165.589	M_p	BnO-/-H, Na$^+$	4103.532	EtO-/-H, Na$^+$
Fe(**3**)OAc (100°C)	4309.453	M_p	BnO-/-H, Na$^+$	4247.401	EtO-/-H, Na$^+$
Fe($\mathbf{6}_{\mathit{meso}}$)OAc (80°C)	4886.517	M_p	BnO-/-H, Na$^+$	-	-
Fe(**8**)OAc (100°C)	5318.840	M_p	BnO-/-H, Na$^+$	5400.940	EtO-/-H, Na
Fe(**10**)OAc (100°C)	4742.440	M_p	BnO-/-H, Na$^+$	4814.844	BnO-/-H, Lactyl, Na

Crystallographic data

Table 2: Selected bond lengths (Å) and angles (°) of Fe(**2**/**3**/**4**/**6**$_{meso}$/**7**/**8**/**10**)OAc.

	Fe(**2**)OAc	Fe(**3**)OAc	Fe(**4**)OAc	Fe(**6**$_{meso}$)OAc	Fe(**7**)OAc	Fe(**8**)OAc	Fe(**10**)OAc
τ	0.65	0.60	0.58	0.58	0.63	0.54	0.59
Fe-O(1)	1.8719(13)	1.8572(18)	1.8729(13)	1.8955(15)	1.900(2)	1.872(2)	1.8978(15)
Fe-O(2)	1.9011(13	1.9046(19)	1.9081(13)	1.8944(15)	1.881(2)	1.859(2)	1.8894(16)
Fe-N(1)	2.2633(17)	2.399(2)	2.2690(15)	2.2726(18)	2.321(3)	2.201(3)	2.0885(19)
Fe-N(2)	2.0716(17)	2.058(2)	2.0828(15)	2.1588(18)	2.177(2)	2.148(3)	2.1224(19)
Fe-O(3)	2.0872(15)	2.0886(19)	2.0826(14)	2.0652(16)	2.080(2)	2.072(2)	2.1124(17)
Fe-O(4)	2.2008(15)	2.145(2)	2.2168(15)	2.2010(15)	2.142(2)	2.353(3)	2.2000(17)
O(1)-Fe-N(2)	111.80(6)	103.39(8)	113.50(6)	100.53(7)	109.76(9)	165.70(11)	123.48(7)
O(1)-Fe-N(1)	89.42(6)	85.84(7)	89.73(6)	88.77(6)	85.92(9)	86.84(10)	85.23(7)
O(2)-Fe-N(1)	165.35(6)	165.42(7)	165.13(6)	168.18(7)	164.53(9)	108.52(11)	158.86(7)
N(1)-Fe-N(2)	78.88(7)	78.80(8)	78.40(6)	79.38(7)	78.71(9)	79.48(10)	76.45(7)
O(1)-Fe-C(acetate)	126.2	129.2	130.56	133.31	126.81	92.52	122.65
O(2)-Fe-C(acetate)	96.78	95.6	96.05	86.41	95.72	133.10	96.51

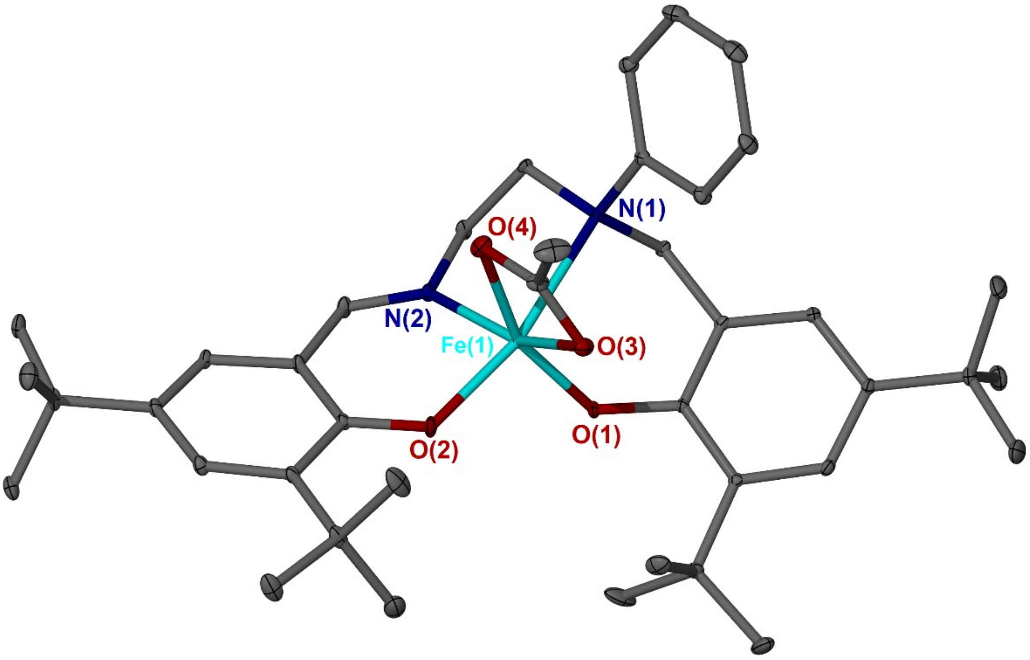

Figure 23: Solid-state structure of Fe(**3**)OAc. Ellipsoids shown at 30% probability level and all hydrogen atoms have been omitted for clarity.

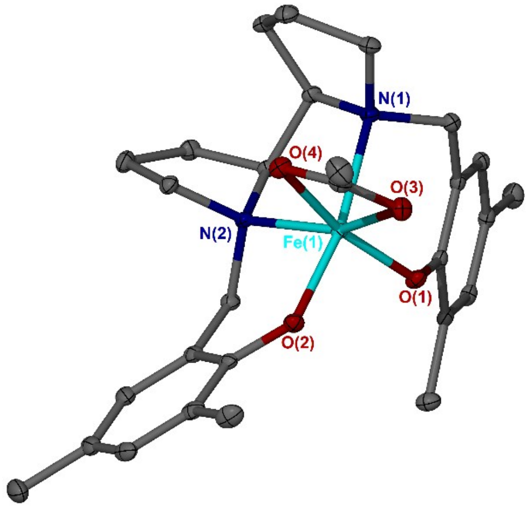

Figure 24: Solid-state structure of Fe($\mathbf{6}_{meso}$)OAc. Ellipsoids shown at 30% probability level and all hydrogen atoms have been omitted for clarity.

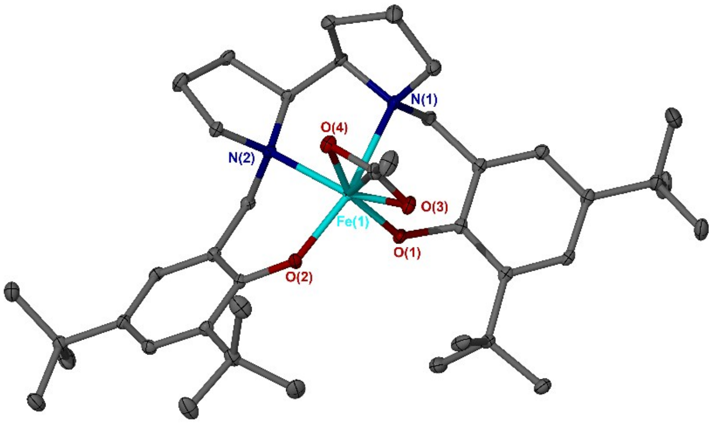

Figure 25: Solid-state structure of Fe(**7**)OAc. Ellipsoids shown at 30% probability level and all hydrogen atoms have been omitted for clarity.

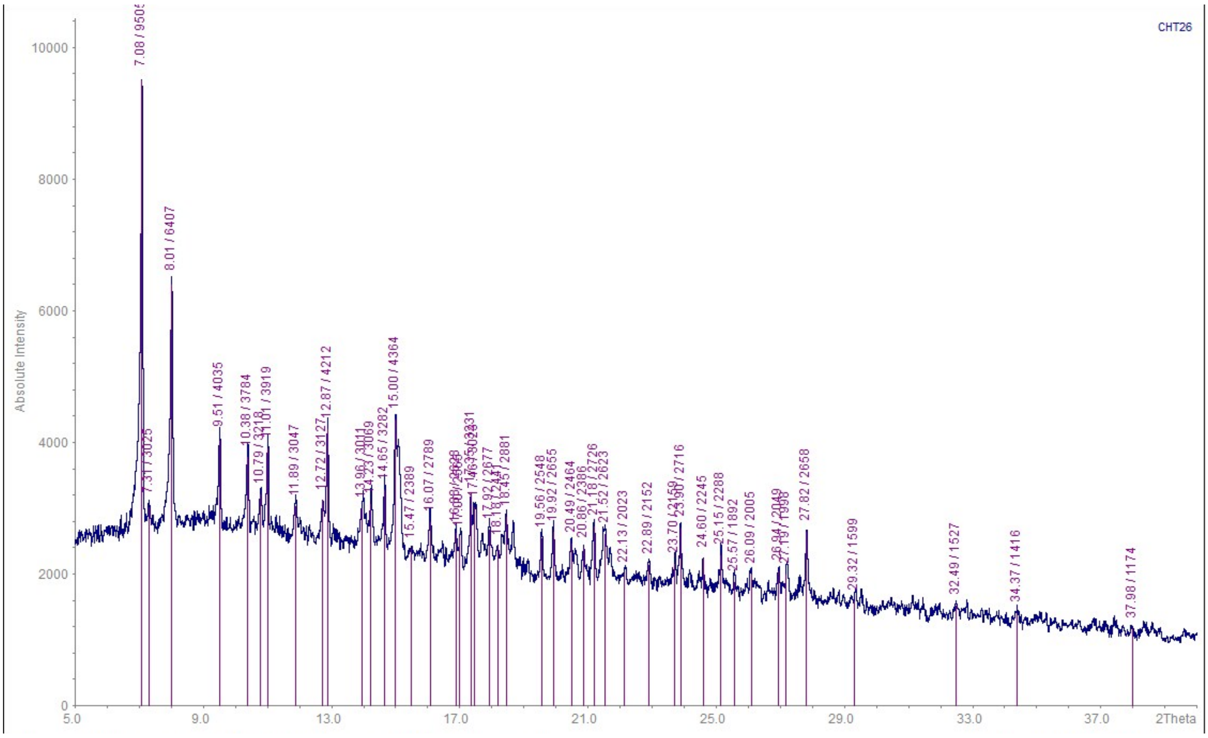

Figure 26: Measured pXRD pattern of Fe(**9**)OAc.

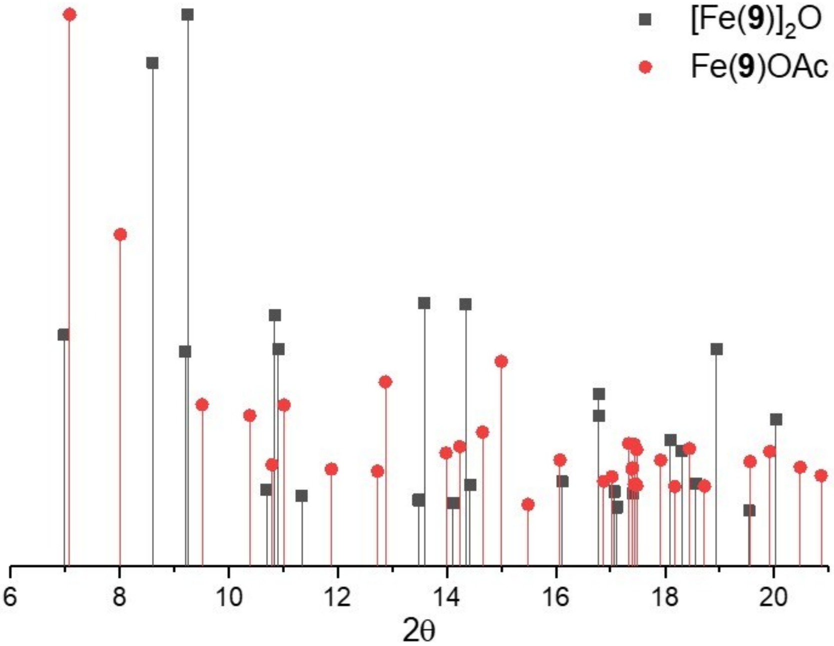

Figure 27: pXRD pattern of Fe(**9**)OAc and generated pattern of [Fe(**9**)]$_2$O.[9] Note – both have been normalised to their most intense reflection.

Table 3 X-ray crystallographic parameters

Compound reference	Fe(**2**)OAc	Fe(**3**)OAc	Fe(**4**)OAc	Fe(**6**$_{meso}$)OAc	Fe(**6**$_{RR}$)OAc	Fe(**7**)OAc	Fe(**8**)OAc	Fe(**10**)OAc
Chemical formula	$C_{37}H_{59}FeN_2O_5$	$C_{42}H_{61}FeN_2O_5$	$C_{38}H_{57}FeN_2O_4$	$C_{28}H_{37}FeN_2O_4$	$C_{30}H_{42.40}FeN_2O_{5.30}$	$C_{40}H_{61}FeN_2O_4$	$C_{38}H_{59}FeN_2O_4$	$C_{34}H_{49}FeN_2O_4$
Formula Mass	667.71	729.77	661.70	521.44	571.71	689.75	663.72	605.60
Crystal system	Monoclinic	Monoclinic	Monoclinic	Monoclinic	Tetragonal	Triclinic	Triclinic	Orthorhombic
a/Å	11.3237(2)	14.7114(3)	10.5080(2)	17.5040(5)	10.24770(10)	10.9269(7)	15.4565(7)	19.0502(18)
b/Å	17.5348(3)	24.5841(4)	22.7778(3)	8.2528(2)	10.24770(10)	13.1291(10)	16.0514(8)	10.2223(6)
c/Å	19.3250(4)	11.2564(2)	15.3749(2)	17.7346(5)	28.1421(5)	14.0182(7)	17.3452(8)	34.8712(12)
α/°	90	90	90	90	90	87.693(5)	86.551(4)	90
β/°	102.572(2)	101.320(2)	91.7990(10)	96.933(3)	90	81.168(4)	86.834(4)	90
γ/°	90	90	90	90	90	80.394(6)	76.058(4)	90
Unit cell volume/Å^3	3745.15(12)	3991.86(13)	3678.15(10)	2543.16(12)	2955.35(8)	1959.1(2)	4165.3(3)	6790.7(8)
Temperature/K	150(2)	150(2)	150(2)	150(2)	150.0(1)	150(2)	150(2)	150(2)
Space group	$P2_1/c$	$P2_1/c$	$P2_1/n$	$P2_1/n$	$P4_12_12$	P**Error!**	P**Error!**	$Pbca$
No. of formula units per unit cell, Z	4	4	4	4	4	2	4	8
Radiation type	Mo Kα	Cu Kα	Cu Kα	Cu Kα	CuKα	Cu Kα	Mo Kα	Mo Kα
No. of reflections measured	34954	29519	28326	17559	79340	12328	43424	66723
No. of independent reflections	7099	7842	6997	4645	2968	6890	14729	5987
R_{int}	0.0581	0.0642	0.0396	0.0393	0.0645	0.0523	0.0770	0.0561
Final R_1 values ($I > 2\sigma(I)$)	0.0405	0.0521	0.0379	0.0374	0.0355	0.0515	0.0651	0.0430
Final $wR(F^2)$ values ($I > 2\sigma(I)$)	0.1052	0.1225	0.0962	0.0938	0.0966	0.1109	0.1259	0.0972
Final R_1 values (all data)	0.0608	0.0754	0.0494	0.0451	0.0392	0.0747	0.1181	0.0585
Final $wR(F^2)$ values (all data)	0.1154	0.1343	0.1010	0.0982	0.0999	0.1194	0.1452	0.1041

References

[1] P. McKeown, M. G. Davidson, J. P. Lowe, M. F. Mahon, L. H. Thomas, T. J. Woodman, M. D. Jones, *Dalton Trans.* **2016**, *45*, 5374–5387.

[2] E. L. Whitelaw, G. Loraine, M. F. Mahon, M. D. Jones, *Dalton Trans.* **2011**, *40*, 11469–11473.

[3] S. M. Kirk, G. Kociok-Köhn, M. D. Jones, *Organometallics* **2016**, *35*, 3837–3843.

[4] O. J. Driscoll, C. K. C. Leung, M. F. Mahon, P. McKeown, M. D. Jones, *Eur. J. Inorg. Chem.* **2018**, 5129–5135.

[5] E. Fazekas, G. S. Nichol, M. P. Shaver, J. A. Garden, *Dalton Trans.* **2018**, *47*, 13106–13112.

[6] D. Alhashmialameer, J. Collins, K. Hattenhauer, F. M. Kerton, *Catal. Sci. Technol.* **2016**, *6*, 5364–5373.

[7] M. Cozzolino, T. Rosen, I. Goldberg, M. Mazzeo, M. Lamberti, *ChemSusChem* **2017**, *10*, 1217–1223.

[8] B. M. Chamberlain, M. Cheng, D. R. Moore, T. M. Ovitt, E. B. Lobkovsky, G. W. Coates, *J. Am. Chem. Soc.* **2001**, *123*, 3229–3238.

[9] K. J. Gallagher, R. L. Webster, *Chem. Commun.* **2014**, *50*, 12109–12111.